Proteomic Analysis of Alzheimer's Disease Models Administered with Rutin and Rutin-Bound Nanoparticles.

By

Alveena Muti

(Registration No: 00000362650)

Department of Biomedical Science

School of Mechanical and Manufacturing Engineering

National University of Sciences & Technology (NUST)

Islamabad, Pakistan

(2024)

Proteomic Analysis of Alzheimer's Disease Models Administered with Rutin and Rutin-Bound Nanoparticles.

By

Alveena Muti

(Registration No: 00000362650)

A thesis submitted to the National University of Sciences and Technology, Islamabad,

in partial fulfillment of the requirements for the degree of

Master of Science in
Biomedical Sciences

Supervisor: Dr. Aneeqa Noor

School of Mechanical and Manufacturing Engineering

National University of Sciences & Technology (NUST)

Islamabad, Pakistan

(2024)

THESIS ACCEPTANCE CERTIFICATE

Certified that final copy of MS/MPhil thesis written by **Regn No. 00000362650 Alveena Muti** of **School of Mechanical & Manufacturing Engineering (SMME)** has been vetted by undersigned, found complete in all respects as per NUST Statues/Regulations, is free of plagiarism, errors, and mistakes and is accepted as partial fulfillment for award of MS/MPhil degree. It is further certified that necessary amendments as pointed out by GEC members of the scholar have also been incorporated in the said thesis titled. **Proteomic Analysis of Alzheimer's Disease Animal Models Administered with Rutin and Rutin-Bound Nanoparticles**

Signature: _____

Name (Supervisor): Aneeqa Noor

Date: 11 - Sep - 2024

Signature (HOD): _____

Date: 11 - Sep - 2024

Signature (DEAN): _____

Date: 11 - Sep - 2024

National University of Sciences & Technology (NUST)

MASTER'S THESIS WORK

We hereby recommend that the dissertation prepared under our supervision by: Alveena Muti (00000362650)
Titled: Proteomic Analysis of Alzheimer's Disease Animal Models Administered with Rutin and Rutin-Bound Nanoparticles be
accepted in partial fulfillment of the requirements for the award of MS in Biomedical Sciences degree.

Examination Committee Members

1.   Name: Muhammad Asim Waris   Signature:

2.   Name: Nosheen Fatima Rana   Signature:

Supervisor: Aneeqa Noor   Signature:

Date: 11 - Sep - 2024

11 - Sep - 2024

Head of Department   Date

COUNTERSINGED

11 - Sep - 2024

Date   Dean/Principal

CERTIFICATE OF APPROVAL

This is to certify that the research work presented in this thesis, entitled "Proteomic Analysis of Alzheimer's Disease Models Administered with Rutin and Rutin-Bound Nanoparticles" was conducted by Ms. Alveena Muti under the supervision of Dr. Aneeqa Noor. No part of this thesis has been submitted anywhere else for any other degree. This thesis is submitted to the Department of Biomedical Sciences (NUST) in partial fulfillment of the requirements for the degree of Master of Science in Field of Neuroscience, Department of Biomedical Sciences, National University of Sciences and Technology, Islamabad.
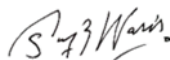
Student Name: Alveena Muti   Signature: _____

Supervisor Name: Dr. Aneeqa Noor   Signature: _____

Name of Dean/HOD: Dr. Asim Waris   Signature: _____

AUTHOR'S DECLARATION

I Alveena Muti hereby state that my MS thesis titled "Proteomic Analysis of Alzheimer's Disease Models Administered with Rutin and Rutin-Bound Nanoparticles" is my work and has not been submitted previously by me for taking any degree from the National University of Sciences and Technology, Islamabad or anywhere else in the country/ world.

At any time if my statement is found to be incorrect even after I graduate, the university has the right to withdraw my MS degree.

Name of Student: Alveena Muti

Date: 11.09.2024

PLAGIARISM UNDERTAKING

I solemnly declare that research work presented in the thesis titled "Proteomic Analysis of Alzheimer's Disease Models Administered with Rutin and Rutin-Bound Nanoparticles" is solely my research work with no significant contribution from any other person. Small contribution/ help wherever taken has been duly acknowledged and that complete thesis has been written by me.

I understand the zero-tolerance policy of the HEC and National University of Sciences and Technology (NUST), Islamabad towards plagiarism. Therefore, I as an author of the above titled thesis declare that no portion of my thesis has been plagiarized and any material used as reference is properly referred/cited.

I undertake that if I am found guilty of any formal plagiarism in the above titled thesis even after award of MS degree, the University reserves the rights to withdraw/revoke my MS degree and that HEC and NUST, Islamabad has the right to publish my name on the HEC/University website on which names of students are placed who submitted plagiarized thesis.

Student Signature: _____

Name: Alveena Muti

"Dedicated to my family, friends and mentors, whose unwavering support, encouragement and guidance have been invaluable throughout this journey. To my dearest siblings, your consistent support has been my strength and inspiration. This achievement is as much yours as it is mine"

ACKNOWLEDGEMENT

I am profoundly grateful to Almighty ALLAH (SWT) for providing me with the strength, patience, and wisdom to complete this research project. Without His guidance, none of this would have been possible. I am deeply grateful to my mother (Amina Bibi), whose love, support, and sacrifices have been the cornerstone of my success. Thank you for always believing in me and encouraging me to pursue my dreams. To my siblings (Sami Ullah, Sana Ullah and Tooba), your constant support and understanding have been a source of comfort throughout this journey.

I am deeply indebted to my supervisor, Dr. Aneeqa Noor, for her continuous support, motivation, and extensive knowledge. Her demonstrative supervision, invaluable guidance, and genuine encouragement have been instrumental in shaping the essence of this research work. I am grateful for the privilege of working under her mentorship.

To my all those friends (Amara Maryam, Amna Hafeez, Faria Hassan, Hina Sajja, Sonia Kiran, Tahreem Mudassar, Maha Adeel, Mehwish Ahsan, Maleeka Khattak, and Zushmalen Afridi) thank you for the laughter, encouragement, and companionship. Your support has been a constant source of motivation, especially during the challenging moments of this journey. I would also like to express my heartfelt appreciation to Mansoor Ali for his unwavering support during challenging times. Your understanding and encouragement when I was feeling down have been invaluable. Your presence has been a great source of comfort and motivation.

Finally, I extend my gratitude to everyone who has supported and believed in me throughout this journey. Your encouragement has made this accomplishment possible.

TABLE OF CONTENTS

LIST OF TABLES

LIST OF FIGURES

LIST OF ABBREVIATIONS AND ACRONYMS

Abbreviation	Full Form
Aβ	Amyloid beta
AD	Alzheimer's Disease
ACh	Acetylcholine
AChE	Acetylcholinesterase
AlCl3	Aluminum Chloride
ANOVA	Analysis of Variance
APP	Amyloid Precursor Protein
AP	Amyloid Plaque
Apo A & E	Apolipoprotein A and E
BBB	Blood Brain Barrier
CAT	Catalase
CDs	Carbon Dots
CNS	Central Nervous System
ChAT	choline acetyltransferase
1-DE	1-Dimensional Gel electrophoresis
dNTPs	Deoxyribonucleotide triphosphate
EAA	Excitatory Amino Acid
H & E	Hematoxylin And Eosin
IL-1B	Interleukin-1B
LC	Liquid Chromatography
MWM	Morris Water Maze
NCBI	NCBI (National Center for Biotechnology and Information)
NCDs	Nitrogen-Dopped Carbon Dots
NF-kß	Nuclear Factor-kß
NFT	Neurofibrillary Tangles
NOR	Novel Object Recognition
NMDA	N-methyl-D-aspartate
PA(%)	Percentage Alteration
PBS	Phosphate-Buffered Saline
PFA	Paraformaldehyde
PL	Photoluminescence
PSEN1	Presenilin 1
PSEN2	Presenilin 2
PTMs	Post Translational Modifications
ROS	Reactive Oxygen Species
Rpm	Revolution per minute
RT	Reverse Transcriptase
RT-PCR	Real-Time polymerase Chain Reaction
SDS-PAGE	Sodium Dodecyl Sulphate Polyacrylamide Gel Electrophoresis
SEM	Standard Error Mean
SEM	Scanning Electron Microscope
SOD2	Superoxide Dismutase 2
ThT	Thioflavin T
TLR4	Toll-Like Receptor 4
VAChT	vesicular acetylcholine transporter

ABSTRACT

Alzheimer's disease is a progressive neurodegenerative disease leading to cognitive impairment and memory loss. The presence of amyloid ß deposition and neurofibrillary tangles remain the neuropathologic criteria for AD diagnosis. The BBB which is necessary for proper neuronal activity prevents solutes from the bloodstream getting into the brain. Unfortunately, there is no effective therapy for the treatment of AD due to low drug potency and various drug delivery issues, such as limited bioavailability and the blood-brain barrier's obstructions. Recently nanotechnology has demonstrated encouraging advancements in the treatment of AD. Many different types of nano-carriers have been modified to provide effective new therapeutic approaches. This study investigated therapeutic effect of Rutin and compared them with those of Rutin-bound nanoparticles, NCDs-Rutin and CDs-Rutin in AD rat model. AD was induced in Wistar Han rats using $AlCl_3$ and D-galactose. The rats were then treated with Rutin and Rutin-bound nanoparticles and the effects were assessed using different parameters. Behavior assessment showed that NCDs-Rutin gave significant results in MWM, Y-maze and NOR test, while CDs-Rutin exhibited better result in open field test. Histological analysis using H & E staining revealed that NCDs-Rutin group prevented brain tissue better than CDs-Rutin and Rutin group, however, Rutin group had more effective amyloid plaque reduction in ThT staining. Moreover, molecular analysis of treatment groups showed an upregulation of SOD2 expression, among them NCDs-Rutin and Rutin group showed significant results suggesting enhanced antioxidant defense. While, CDs-Rutin group showed significant reduction in TLR4 expression, suggesting a reduced neuroinflammation. Proteomic analysis through SDS-PAGE indicated differences protein expression across the groups. The Rutin-bound nanoparticles significantly outperformed Rutin in terms of efficacy, most likely as a result of their focused administration and increased bioavailability.

Keywords: Alzheimer's Disease, Carbon Dots, Cholinergic System, Nanoparticles, Nitrogen-Doped Carbon Dots, Rutin.

CHAPTER 1: INTRODUCTION

The development of cognitive and behavioral impairment in neurological diseases is known as AD. Traditional treatment methods, such as acetylcholinesterase inhibitors, frequently don't work since they're not soluble enough, have a low bioavailability, and don't obstruct the blood and brain flow. This disease is the most prevalent type of dementia and one of the major worldwide health issues. It is a neurological disease that gradually impairs cognitive function and causes memory loss (Ballard et al., 2011). Nanotechnology has lately found a possible area of study for AD treatment. Since AD is one of the oldest diseases and less than 5% of cases are directly inherited, environmental variables may be crucial in both the early stages and progression of the disease. Clinical enhancing nano-systems are designed, characterized, developed, and put into use as part of nano-technological approaches to healthcare (Fonseca-Santos et al., 2015). Aβ accumulated in the brain would be a factor in pathogenic AD pathways. Despite appearing to be mostly found in neurons, beta-amyloid production can take many different chemical forms. Due to the difficulty of crossing the BBB at the nanoparticle level, particles will traverse it without requiring sophisticated modification in the 50–100 nm range. For every nanoparticle derivative, a therapeutic solution is advised if there is a limit to the BBB's crossing. (Ordóñez-Gutiérrez & Wandosell, 2020). The discovery of CDs has led to several firsts in recent years, including the delivery of medication through the blood-brain barrier. CDs are harmless and biocompatible since they don't contain any metals. Because of their many surface functional groups, CDs can be conjugated, as a nanocarrier, with a variety of medicinal compounds through covalent or noncovalent interactions.

1.1. Alzheimer's Disease

AD, named after the German psychiatrist Alois Alzheimer, is the most common type of dementia. It is described as a progressive neurodegenerative disease caused by the build-up of amyloid-beta peptide (Aβ) in the brain's most affected area, the medial temporal lobe and neocortical structures, which results in neuritic plaques and neurofibrillary tangles (De-Paula et al., 2012). Alois Alzheimer noticed amyloid plaques and a significant loss of neurons in the brain of his first patient, who had memory loss and change in personality before to passing away. He described the patient's ailment as a horrible cerebral cortex disease. Initial memory loss and cognitive decline are the most prevalent features, and these can later affect motor

function, speech, behavior, and visuospatial orientation (Cipriani et al., 2011). Brain disorders such as AD or other conditions such as infections, intoxications, abnormalities in the pulmonary and circulatory systems that reduce the amount of oxygen reaching the brain, tumors, and so on can all lead to a progressive loss of cognitive functions (Livingston et al., 2020).

1.2. Epidemiology of AD

AD is a major cause of mortality because dementia causes progressive cognitive impairment that interferes with daily functioning. It is believed that 44 million individuals globally suffer from dementia at present time. This is predicted to more than triple by 2050 as the population ages, and dementia could cost the US economy more than US$600 billion a year in only the USA (Prince et al., 2014). In Europe as a whole, accounting for 10.7% of mortality rate recorded in 2014. Global statistics indicate that 4% of persons older than 60 years suffer from dementia. 2.1% in Africa, 4.0% in China and the Western Pacific, 4.6% in Latin America, 5.4% in Western Europe, and 6.4% in North America were the regional prevalence rates (Ferri et al., 2005). The 5 million new cases of dementia that are detected each year, the most of which have AD, affect over 25 million individuals globally (Brookmeyer et al., 2007). Every 20 years, there is expected to be a rise in dementia cases. In developed nations, approximately one-third of the very old may have dementia-related symptoms and indications, while one in ten elderly people suffer from dementia to some degree.

The two most prevalent forms of dementia, AD and vascular dementia, account for 20% to 30% and 40% to 80% of all dementia cases, respectively. Subtypes of dementia are similar globally (Corrada et al., 2008). Individually, AD significantly reduces life expectancy and is a major contributor to physical impairment, institutionalization, and a decline in the standard of living for the elderly. First, institutionalization and functional disability are closely linked to AD. An estimated 11.2% of years spent incapacitated among persons over 60 are attributed to dementia, against 9.5% for stroke, 8.9% for musculoskeletal disorders, and 5.0% for cardiovascular diseases (Qiu et al., 2009).

1.3. Neuropathology of AD

The cytoskeletal changes brought on by the aberrant tau protein production in a few vulnerable neuronal subtypes are the defining feature of AD. The tau protein in healthy nerve cells stabilizes the neuronal cytoskeleton's microtubules, which are crucial in the movement of

materials between different cell compartments. Impaired signaling by retrograde neurotrophic factors, incorrect protein metabolism, and synaptic dysfunction are likely caused by aberrant tau protein production, destabilizing microtubules, and obstructing axonal transport. The affected neurons may die largely as a result of a decline in their functions (Perl, 2010). In addition to "negative" lesions like neuronal and synaptic loss, the neuropathology of AD also includes "positive" lesions such amyloid plaques and cerebral amyloid angiopathy, neurofibrillary tangles, and glial responses. Due to losses in synapses, neuropils, and neurons, negative lesions show significant atrophy. Moreover, oxidative stress, neuroinflammation, and harm to cholinergic neurons can potentially cause neurodegeneration (Spires-Jones & Hyman, 2014).

1.3.1. Senile plaques

The other main pathological lesion observed in people with AD is the senile or neuritic plaque. Senile plaques are complex structures that have an accumulation of the 4-kD beta-pleated sheet-shaped protein βA4 in the center. Individuals with AD and the elderly may also have various forms of plaques in their brains that include βA4 (Šimić et al., 2017). Extracellular deposits of Aβ protein, referred to as senile plaques, can exhibit many morphological characteristics, including neuritic, diffuse, dense-cored, classic, or compact type plaques. Proteolytic cleavage-prone enzymes such as β- and γ-secretase are responsible for synthesizing Aβ deposits from the transmembrane APP (Cras et al., 1991). The final forms of Aβ40 and Aβ42 are produced by combining the amino acid fragments (43, 45, 46, 48, 49, and 51) that are produced when these enzymes break down APP. There are two types of Aβ monomers: large insoluble amyloid fibrils that can accumulate to produce amyloid plaques and soluble oligomers that can multiply throughout the brain. Thickened plaque accumulation in the different parts of the brain can induce cognitive impairments because Aβ is involved in neurotoxicity and neuronal function (Chen et al., 2017).

1.3.2. Neurofibrillary Tangles (NFT)

One important neuropathological characteristic of AD is neurofibrillary tangles. Neurons producing NFT have been found to exhibit the loss of cytoskeletal microtubules and tubulin-associated proteins. It is believed that protein phosphorylation and dephosphorylation involved in signal transduction generate neurofibrillary lesions, although the exact biochemical mechanisms connecting the loss of cytoskeletal components to the formation of NFT remain

unclear. For instance, the main component of NFTs, tau, is abnormally phosphorylated (hyperphosphorylated) in patients diagnosed with AD compared to those of non-demented people (Zempel & Mandelkow, 2014). The reason of tau's missorting in neurons during AD is believed to be epitope-specific hyperphosphorylation, which causes the protein to move from a mostly axonal to a somato dendritic position (Alonso et al., 2008). Hyperphosphorylated tau protein aberrant filaments, or NFT, have the ability to coil around one another to form paired helical filaments (PHF) at specific phases. These filaments accumulate in the cytoplasm of axons, dendrites, and neural perikaryal cells. This results in the degeneration of cytoskeletal microtubules and tubulin-associated proteins (Metaxas & Kempf, 2016).

1.3.3. Synaptic Loss

Synapse loss causes abnormalities in sensory, motor, and cognitive functions in a number of neurodegenerative disorders, such as major depressive disorder, schizophrenia, AD, Huntington's disease, amyotrophic lateral sclerosis, and aging. The loss of excitatory synapses is the most important indicator of cognitive deterioration in AD (Henstridge et al., 2016). Early-stage AD is usually accompanied by synapse loss in the limbic system and neo-cortex, which impairs memory. Synaptic loss pathways include defects in axonal transport, oxidative stress, mitochondrial damage, and other events that may result in tiny fractions, like tau and Aβ buildup at the synaptic locations. The end products of these processes include dendritic spine loss, axonal degeneration, and pre-synaptic terminals (Overk & Masliah, 2014). Synaptic proteins that serve as biomarkers for the identification of synaptic loss and severity include neurogranin, a postsynaptic neuronal protein, and synaptotagmin-1 (Lleó et al., 2019).

1.4. Stages of AD

Four stages make up the clinical phases of AD: the pre-clinical phase, also known as the pre-symptomatic stage, can extend over a number of years. There are now no early pathological abnormalities in the cortex and hippocampus, no mild memory loss, no functional impairment in day-to-day activities, and no clinical indicators or symptoms of AD (Dubois et al., 2016). The moderate or early stage of AD is when many symptoms first appear in patients. These symptoms include mood swings, the beginning of depression, difficulty adjusting to daily life owing to memory loss and attention challenges, and confusion regarding place and time (Wattmo et al., 2016). When AD reaches a moderate stage, it affects more brain regions, causes more severe memory loss that makes it difficult to recall friends and family, impairs

impulse control, and makes it difficult to read, write, and talk (Kumar et al., 2021). Severe AD, also known as late-stage AD, is characterized by a progressive loss of function and cognition, which includes the inability to recognize family members, bedridden status, difficulty ingesting and urinating, and ultimately death from these challenges. A substantial collection of the disease called neurofibrillary tangles and neurotic plaques extended throughout the entire cortical area (Apostolova, 2016).

1.5. Causes and Risk Factor

AD is a multifactorial disease that is impacted by several risk factors, including vascular problems, infections, aging, genetics, head trauma, and environmental factors like heavy and trace metals, as seen in Figure 1.1. The pathogenic changes (Aβ, NFTs, and synaptic loss) linked to AD are presently unknown in their cause. Although there are numerous ideas to explain AD, only two are regarded as major: one contends that cholinergic dysfunction is a key risk factor, while the other suggests that changes in the generation and processing of amyloid β-protein are the primary cause of the illness. However, as of yet, no accepted theory has been established to explain the pathophysiology of AD (A. Armstrong, 2019).
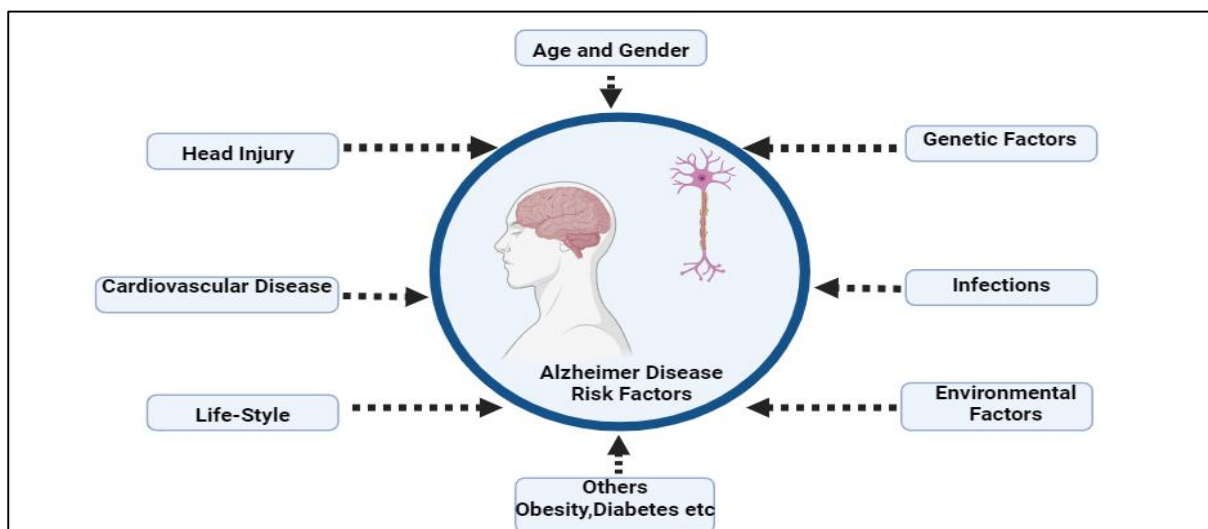
Figure 0.1: Risk factors of AD. It is influenced by a combination of factors, from genetics and age, infections in the body, cardiovascular diseases, head injuries and tumors to lifestyle and environmental exposures.

1.5.1. Cholinergic Hypothesis

Acetylcholine is produced by the enzyme choline acetyltransferase (ChAT), which was linked to abnormalities in neocortical and presynaptic cholinergic function in the 1970s. Because of its importance to cognitive function, the cholinergic hypothesis of AD was put

forth. The ChAT enzyme converts choline and acetyl-coenzyme A into ACh in the cytoplasm of cholinergic neurons. The VAChT then carries the ACh to the synaptic vesicles (Figure 1.2). In the brain, ACh is essential for several physiological functions, including learning, memory, attention, and sensory processing. One of the main characteristics of AD has been identified as cholinergic neuron degeneration, which results in changes in cognitive function and memory loss. It is believed that Aß reduces choline absorption and releases ACh by interfering with cholinergic neurotransmission (H. Ferreira-Vieira et al., 2016).

The results of studies showed a relationship between the generation of amyloid fibrils and cholinergic synaptic loss, as well as between the neurotoxicity of Aβ oligomers and the interactions between AChE and Aβ peptide. Further factors that contribute to the progression of AD include a decrease in excitatory amino acid (EAA) neurotransmission, where glutamate concentration and D-aspartate uptake are significantly reduced in many cortical areas in AD brains, as well as a reduction in nicotinic and muscarinic (M2) ACh receptors, which are found on presynaptic cholinergic terminals. Additionally, cholinergic receptor antagonists, such as scopolamine are also employed; these drugs have been demonstrated to induce amnesia. This effect can be reversed by substances that stimulate the synthesis of ACh. Thus, the cholinergic hypothesis is predicated on the following: the decline in presynaptic cholinergic markers in the cerebral cortex; the source of cortical cholinergic innervation; the severe neurodegeneration of the nucleus basalis of Meynert (NBM) in the basal forebrain; and the comparative role of cholinergic antagonists and agonists in memory decline (Hampel et al., 2018).

1.5.2. Amyloid Hypothesis

The amyloid hypothesis was first proposed some decades ago when it was discovered that dementia has a strong correlation with abnormal β-sheet deposition in the central nervous system. However, it was found that normal, healthy brains also acquire amyloid plaques (AP) during aging. This result raised the question of whether or not AP deposition is the root cause of AD. Consequently, other hypotheses have been proposed recently for the non-inherited form of AD (NIAD); nonetheless, the amyloid hypothesis remains the most commonly acknowledged pathogenic mechanism for hereditary AD (IAD) (Paroni et al., 2019). According to the amyloid hypothesis, age and illness reduce the quantity of β- and γ-secretase, which breaks down Aβ that is formed from APP. Consequently, Aβ peptides, specifically Aβ40 and Aβ42, build up. Aβ amyloid fibrils are produced when the ratio of Aβ42/Aβ40 rises, and these fibrils cause tau pathology, neurotoxicity, neurodegeneration, and neuronal cell death. There

have been reports of Aβ catabolism and anabolism being impacted by risk factors for AD and mutations in a number of genes, including APP, PSEN1, and PSEN2. As a result, there is an accumulation of Aβ and neurodegeneration advances quickly (Kametani & Hasegawa, 2018).
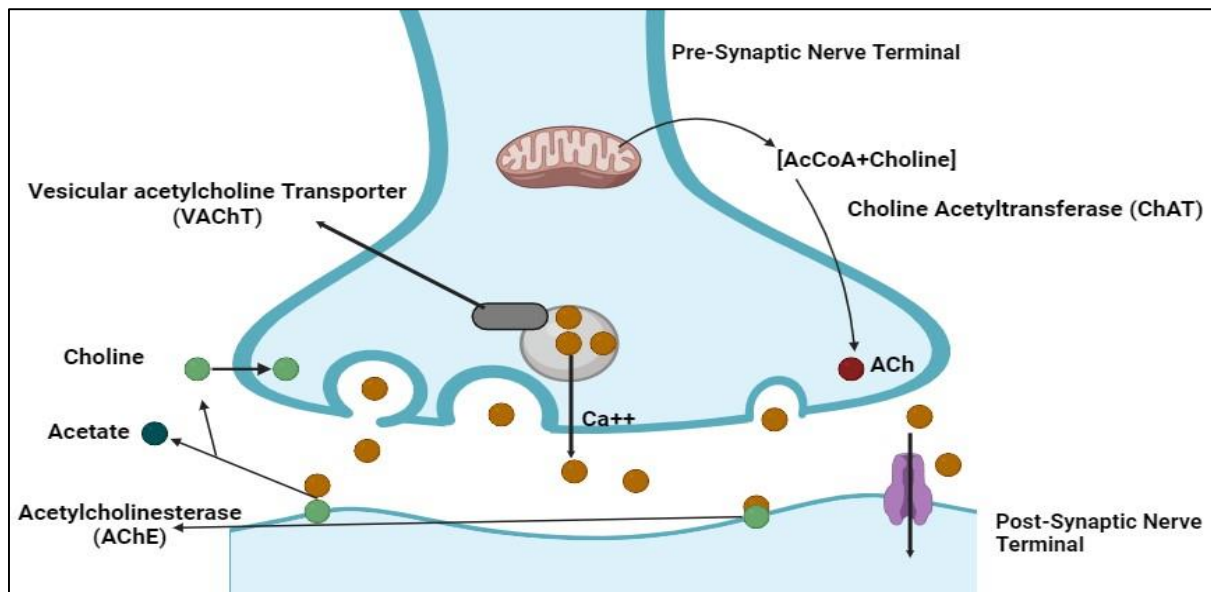
Figure 0.2: Role of Acetylcholine in Synaptic Transmission. It is highlighting the synthesis of ACh by ChAT and the breakdown of ACh by AChE.

1.6. Treatment and Limitations

In order to slow the course of cognitive symptoms as well as behavioral and psychosocial symptoms of dementia, current medication treatments for AD are symptomatic rather than curative. Four medications, galantamine, rivastigmine, memantine, and donepezil belong to the anticholinesterase inhibitor and anti-glutaminergic groups and are authorized for sale. These medications are administered orally or topically (Livingston et al., 2019).

1.6.1. Mechanism of Action and Classification of Approved Drugs

The purpose of anticholinesterase inhibitors is to raise the brain's ACh levels, which are involved in memory and information transfer between specific neurons. The goal of these therapies is to address the ACh shortage seen in AD patients' central nervous systems. N-methyl-D-aspartate (NMDA) receptors have a noncompetitive antagonist action that is exploited by anti-glutaminergics to control glutamate levels. A neurotransmitter called glutamate is involved in learning and memory processes in the brain. Elevated glutamate is probably going to have pathogenic effects, including neuronal death. These medication-based therapies aim to slow down the progression of the disease, stabilize or temporarily enhance cognitive abilities, and manage behavioral issues. These therapies assist AD patients and their

carers maintain their independence and enhance their quality of life, even though they are not curative. But these therapies simply address the symptoms of AD rather than its underlying cause, and their efficacy is only marginal at best (Cummings et al., 2018).

In the early asymptomatic phase, these pharmacological treatments may be more beneficial before the process of neurodegeneration starts. One of the main aspects that contributes to the low effectiveness of the treatments is the difficulty in targeting brain medications because of the restricted transit from the circulation to the CNS through BBB. In fact, many drug trials for AD are unsuccessful due to permeability issues at the BBB (Zenaro et al., 2017).

This calls for a greater dosage, which could increase the possibility of more unfavorable effects. The BBB presents a challenge for CNS medication delivery, to which several approaches have been proposed and implemented. Drug efficacy may be lowered by preclinical research's possible failure to account for age-related changes in neuronal membranes and membrane receptors. Indeed, a recent study found changes in the microdomains of synaptosomes taken from aged mice, making them more susceptible to amyloid stress and impeding the neuroprotective effects of ciliary neurotrophic factor (Colin et al., 2017). Since AD is difficult to diagnose in its early stages and there are currently no effective curative treatments, it is critical to take neuroprotective and preventive measures to slow down the neurodegenerative process and neuronal dysfunctions, including axons, dendrites, and synapses, as well as lower the risk of AD (Klimova & Kuca, 2015).

1.7. Role of Nanotechnology in AD

1.7.1. Drug Delivery Challenges Treatment of AD

The treatment for AD involves the administration of drugs orally. Although oral administration is convenient for patients, there are a number of obstacles that must be overcome in order to achieve the desired outcomes, including poor bioavailability, first-pass metabolism, limited absorption, and dose-dependent side effects. Targeting the brain also involves added issues with the BBB. It is a unique and complex multicellular structural barrier that separates body's tissues from the central nervous system. It is composed of a semi-permeable endothelial cell membrane (Yiannopoulou & Papageorgiou, 2020). In the human body, the BBB is the most tightly regulated biological barrier. It shields the brain against harmful substances and blood-borne diseases while preventing viruses and the majority of macromolecules from

entering the central nervous system. However, the difficulties in getting a range of potentially beneficial chemicals into the brain outweigh the BBB's obvious benefits (Goedert & Spillantini, 2006).

1.7.2. *Blood-Brain-Barrier: Barrier to Effective Treatment*

One efficient technique to get across the blood-brain barrier is to load drugs within nanocontainers, which are defined by their relatively small size and ability to overcome the barrier. This method of delivering medication helps to maximize the bioavailability of pharmaceuticals while reducing the likelihood of side effects. Nano-formulations are characterized by their controlled release of active pharmacological ingredients, flexibility, altered surface properties, and plasticity. They target CNS active drugs to the brain through the blood-brain barrier (Agrahari, 2017).

Additionally, research shows that nano-technological methods hold great promise for the development of successful brain-targeted therapies and can improve treatment efficacy and early AD diagnosis. One of the most innovative and promising nanocarriers with potential uses in nanomedicine is CDs. They are relatively simple to synthesise and have a number of beneficial characteristics, including tunable photoluminescence (PL), chemical stability, low cytotoxicity, good photostability, and exceptional biocompatibility (Zhang et al., 2021). Furthermore, CDs have the potential to be a highly developed medication delivery technology that can traverse the blood-brain barrier. CDs are typically spherical or hemispherical, with a core composed mostly of sp2 inter-hybridized carbon atoms. Their size is less than 10 nm. CDs have a complex structure and form due to the abundance of functional groups on their surface. Furthermore, a wide range of polymer chains and surface groups, such as amine, hydroxyl, and carboxyl, improve water solubility, making it simple to combine with other materials without phase separation (Mansuriya & Altintas, 2021).

1.8. Rutin

One of the primary plant phytochemicals that are active is flavonoids, which are well-known for their antioxidant and membrane-stabilizing qualities. Plants and their parts, especially citrus fruits like lemon, orange, lime, and grapefruit, contain Rutin. Other sources include buckwheat, asparagus, mulberry and rue berries. One of the most popular dietary flavonoids that people regularly ingest is Rutin, which can be found in fruits, vegetables, and plant-based liquids like wine and tea (Yang et al., 2008a). Rat tissues exposed to a greater dose

of Rutin (1%) for 20 days displayed an enhanced level of liver antioxidant in the rats. In other situations, though, it lowers minerals and inhibits the actions of some metal-containing enzymes that might be detrimental to health. Rutin and other supplements were tested on Wistar rats, and the results showed that they decreased oxidative stress and systemic inflammation (Mosoni et al., 2010). Rutin may be advantageous to the muscle protein metabolism throughout aging, according to research on the impact of Rutin and other supplements on the leucine-regulated protein metabolism in the muscles of adult and elderly rats (Marzani et al., 2008).
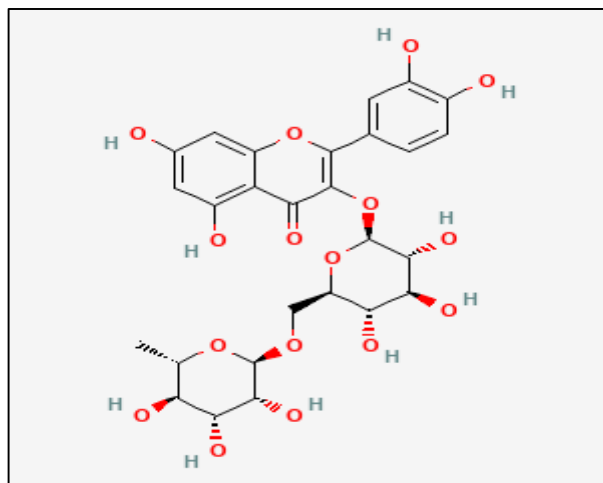
Figure 0.3: **Chemical structure of Rutin** contains hydroxy group at carbon 3 attached with glucose and rhamnose sugar group. PubChem ID: 5280805

1.8.1. Pharmacological Properties of Rutin

Known by several names such as sophorin, rutoside, and quercetin-3-Rutinoside, Rutin (3,3,4,5,7-pentahydroxyflavone-3-rhamnoglucoside) is a polyphenolic bioflavonoid that is mostly obtained from organic sources. Ruta graveolens, a plant that also includes Rutin and is a vital component of plant nutrition, is the source of the word "Rutin." In terms of chemistry, it is a glycoside composed of the flavonoid quercetin and the disaccharide Rutinose. Some studies suggest that Rutin may protect against NDs because of its beneficial qualities as a potent antioxidant (Yu et al., 2015). Rutin has been shown to have a wide range of therapeutic applications because of its various qualities, which include antioxidant, anti-inflammatory, cardiovascular, neuroprotective, antidiabetic, and anticancer effects. Over time, numerous pathways in both *in vitro* and *in vivo* models have been associated with its antioxidant capabilities. First, it was mentioned that the chemical structure of ROS might allow for direct scavenging. Secondly, it increases the synthesis of glutathione and is believed to increase the expression of several antioxidant enzymes, such as SOD and CAT, which in turn upregulates

the oxidative defense mechanisms of cells. Thirdly, Rutin inhibits xanthine oxidase, which stops ROS from being produced. (Hanasaki et al., 1994).

1.8.2. *Mechanism of Action*

The blood-brain barrier is a tight junction that can be crossed by Rutin and/or its metabolites. Rutin is also utilized to display different demeanor symptoms associated with neurodevelopmental disorders. Its antioxidative and anti-inflammatory properties help to Rutin reduces the effects of diabetes, obesity, and AD (Habtemariam, 2016). Rutin reduces the synthesis of nitric oxide, inhibits Aβ aggregation and cytotoxicity, reduces the generation of proinflammatory cytokines, and lessens oxidative stress. It is generally considered safe and ingested through diet. Research suggested that Rutin had several impacts at once. It preserves neuronal morphology against hazardous tau oligomers, prevents tau aggregation and tau oligomer-induced cytotoxicity, reduces the synthesis of proinflammatory cytokines, and increases microglial absorption of extracellular tau oligomers *in vitro* (Sun et al., 2021).

It reduced TNF-α and IL-1β production in microglia, which in turn inhibited the action of proinflammatory cytokines. The suppression of β-amyloid oligomeric cytotoxicity indicates that this effect may be helpful in the treatment of AD (Wang et al., 2012). By reducing the activity of the glial fibrillary acidic protein, interleukin-8, cyclooxygenase-2, inducible nitric oxide synthase, and nuclear factor-kß, Rutin attenuated streptozotocin-induced inflammation and consequently averted gross morphological alterations in the rat hippocampal region. Such an effect shows promise in treating "sporadic dementia of Alzheimer type" and may be helpful in preventing cognitive deficits (Javed et al., 2012). Moreover, it has various other pathological effects.

1.8.2.1. *Antioxidant Activity*

With its capacity to cause neuronal damage and encourage the creation of harmful amyloid-beta (Aβ) clumps, oxidative stress is a key factor in the onset and progression of AD. Conversely, Rutin demonstrates strong antioxidant properties through its ability to scavenge free radicals and lessen oxidative damage to neural cells. Moreover, Rutin increases the activity of innate antioxidant enzymes like catalase and superoxide dismutase (SOD), protecting neurons from oxidative damage (Yang et al., 2008b).

1.8.2.2.   Anti-inflammatory Effects

Chronic neuroinflammation, characterized by the activation of microglial cells and the release of pro-inflammatory cytokines including interleukin-1β and tumor necrosis α, is another significant aspect of AD pathology. Rutin blocks the synthesis of pro-inflammatory mediators and stops microglia from activating, which is how it demonstrates its anti-inflammatory qualities. Moreover, Rutin dramatically lowers neuroinflammation in AD via modifying the signaling pathway for nuclear factor-kappa B (NF-κB) (Xu et al., 2014).

1.8.2.3.   Neuroprotective Effects

In AD, Rutin's capacity to maintain neuronal survival and function serves as evidence of its neuroprotective properties. By encouraging neurogenesis and synaptic plasticity, two processes that are compromised in AD brains, Rutin aids in the survival of neurons. Furthermore, Rutin prevents neuronal apoptosis by influencing apoptotic signaling pathways like caspases and the Bcl-2 family of proteins. Additionally, Rutin stops Aβ peptides from clumping together to form hazardous oligomers and fibrils, which lessens the neurotoxicity that Aβ causes in AD (Budzynska et al., 2019).

1.9.   AD Related Abnormalities in Proteomics

Since the earliest days of biological inquiry, the dynamic role that molecules play in supporting life has been observed. In 1838, Berzelius gave these molecules the label "protein," which comes from the Greek word proteios, which means "the first rank," to emphasize their significance. The term "proteome" refers to the total number of proteins in a cell that are characterized at any one time by their turnover, post-translational modifications, interactions, and localization. The term "proteomics" was first used in 1996 by Marc Wilkins to describe the "PROTein complement of a genOME " (Cristea et al., 2004). Early and accurate diagnosis of AD is essential for implementing timely interventions and developing effective therapeutic strategies. Proteomic biomarkers, as shown in figure 1.4, are associated with disease that can be used to monitor and diagnose different phases of the disease as well as identify potential treatment targets or therapeutic response candidates. The body's tissues and biofluids exhibit altered protein expressions as the disease progresses, providing early warning signs of the disease (Jain et al., 2023). There are various proteins from different categories, among which

few are upregulated while others showing downregulation, are involved in AD pathogenesis, as in figure 1.4.
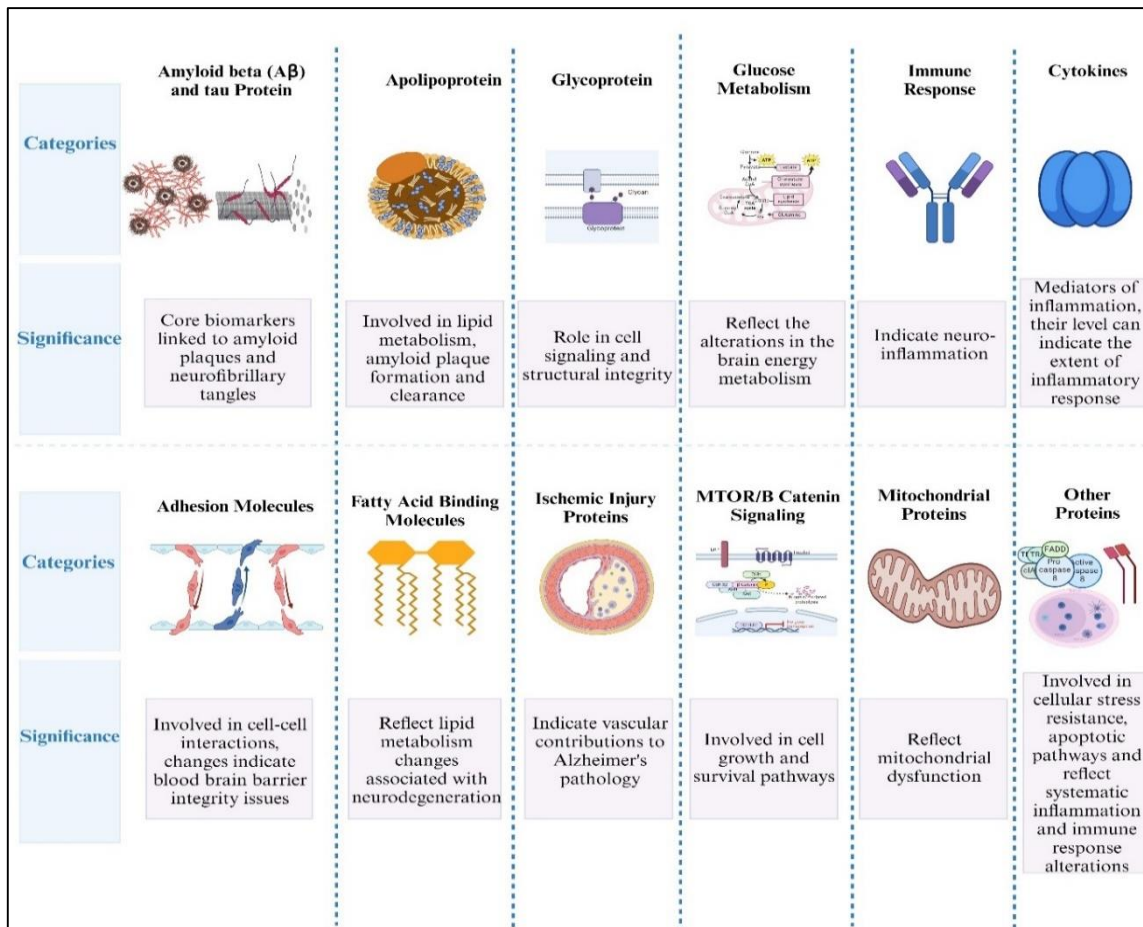
Figure 0.4: **An overview of the major categories** and their importance in comprehending the disease mechanisms of protein biomarkers linked to Alzheimer's disease, highlighting their roles in amyloid pathology, glycoproteins, lipid metabolism, cell signaling, inflammation and brain metabolism. These biomarkers give insightsinto disease mechanisms, potential diagnostics and therapeutic targets.

1.9.1. Aβ and tau protein

Aβ is synthesized from amyloid precursor protein (APP) by a series of cleavages involving β-secretase and γ-secretase. The buildup of Aβ in amyloid plaques inside the brain, as well as disruptions in the proteolytic degradation of APP and the discharge of Aβ peptides, are significant occurrences in the development of AD (Sun et al., 2015). Tau protein is largely found in neurons and stabilization of microtubules within the brain is one of its many functions. Neurofibrillary tangles, which are composed of abnormal tau protein, are a characteristic hallmark of AD. Owing to their significant contribution in AD pathology, studies have shown higher quantities of Aβ42, reduced or unaltered concentrations of Aβ40, and higher concentrations of tau in subjects with AD (Tatebe et al., 2017).

1.9.2. *Apolipoproteins*

ApoA and E is a class of proteins essential for cholesterol and lipid metabolism. They play a crucial role in lipoprotein assembly, solubilizing lipid fractions into lipoproteins, receptor binding, and the function of lipid transport enzymes. By regulating lipid distribution between lipoproteins and tissues, apolipoproteins help stabilize blood lipid levels. Recent studies suggest that level of both ApoA and E was low in AD patients (Kitamura et al., 2017).

1.9.3. *Glycoproteins*

Glycoproteins like feutin A and B are primarily produced in hepatocytes, is ubiquitous in blood, and achieves standard serum levels shortly after birth. It is mostly exhibited by adult liver cells and embryonic cells, with fewer expression in monocytes and adipocytes. Fetuin-A and B demonstrates a wide range of pathological and physiological functions, including neuroprotective and anti-inflammatory effects. According to the findings, concentrations of both found in the bloodstreams of mild AD patients were considerably downregulated than in healthy individuals (Ricken et al., 2022).

Aim of the Study

Understanding Rutin's neuroprotective properties and developing a treatment plan for AD will require further research on the use of Rutin and Rutin-bound NPs in various AD models. Therefore, Rutin, which possesses anti-inflammatory and antioxidant properties, might be able to reduce the effects of AD when paired with nanoparticles, particularly CDs and NCDs. The findings of this study would help to clarify how Rutin and Rutin-bound nanoparticles work to improve cognitive performance, prevent neurodegeneration, and control proteome alterations associated with AD. The understanding of Rutin's pharmacodynamics, dosage, and therapeutic uses in the treatment of Alzheimer's disorders may be facilitated by more research on the drug and its nanoparticle systems. The aims and objectives of this study are as follows:

- Establishment of Alzheimer's disease in animal models by employing D-galactose and $AlCl_3$
- Administration of Rutin and Rutin-bound nanoparticles are optimized to reduce the effects of Alzheimer's
- Behavioral, histopathological, molecular and proteomic analysis to assess molecular alterations and cognitive enhancement

CHAPTER 2: MATERIALS AND METHODOLOGY

2.1. Ethical Approval

Ethical approval (IRB no. 05-2023-ASAB-02/02) was acquired from the NUST-IRB committee of the National University of Sciences and Technology, Islamabad before conducting *in vivo* study.

2.2. Experimental Design

In this study, male Wistar Han rats of similar age and health were used to assess the effectiveness of Rutin and Rutin-bound nanoparticles in mitigating the effects of AD. After then, AD was induced over a period of ten days using a mixture of $AlCl_3$ and D-galactose to cause the condition. This approach was created to simulate both the behavioral and clinical characteristics linked to AD in humans. Following this induction phase, the rats' fundamental motor and cognitive, spatial abilities were assessed behavior testing. When the treatment period ended, the rats were dissected in accordance with experimental ethics protocols, and the brains were removed to get the necessary brain regions such as the cortex for proteomic and molecular research. Polymerase chain reaction (PCR) identification utilizing SOD2 and TLR4 gene-specific primers was the first step in the molecular study. In order to do SDS-PAGE analysis, proteins were extracted from brain tissues using a lysis solution containing protease inhibitors, and the concentration of each protein was then measured. The experimental design and timeline for the study is shown in figure 2.1. Every experiment carried out for this thesis was done so under an IACUC authorization and in strict accordance with the National Research Act and the Animal Welfare Act regarding the use of animals in research.

2.3. Animals and Disease Induction

Adult male Wistar Hans rats, weighing 290 ± 20 g and aged between 8 to 12 months, were acquired and kept in the animal house of the Atta-ur-Rahman School of Applied Biosciences (ASAB), National University of Sciences & Technology (NUST), Islamabad. The environment was carefully maintained, with a temperature range of $25 \pm 2°C$. Prior to the treatment, the rats were housed for seven days to allow them to get used to their surroundings. Throughout the trial, each group was kept in a single cage in rooms with controlled humidity and temperature. The 14-hour light and 10-hour dark cycles of natural light and dark were observed.

The animals were divided into five groups at random before the commencement of dosing so that the mean body weight of each group was almost equal. There were four animals in each group. For the duration of the 15-day research, Group 1 animals received filtered water orally and were maintained as normal controls (NC). For disease induction, AD was induced in rats using a combination of $AlCl_3$ and D-glactose dissolved in PBS. This mixture was administered to the rats via intra-peritoneal injection for one week. $AlCl_3$ and D-galactose were dissolved separately in PBS before being combined. The dosage was adjusted based on the weight of each rat, and administrations were performed daily. This induction method was chosen to mimic pathological features observed in AD models. Throughout the induction period, rats were closely monitored for any signs of distress or adverse effects.
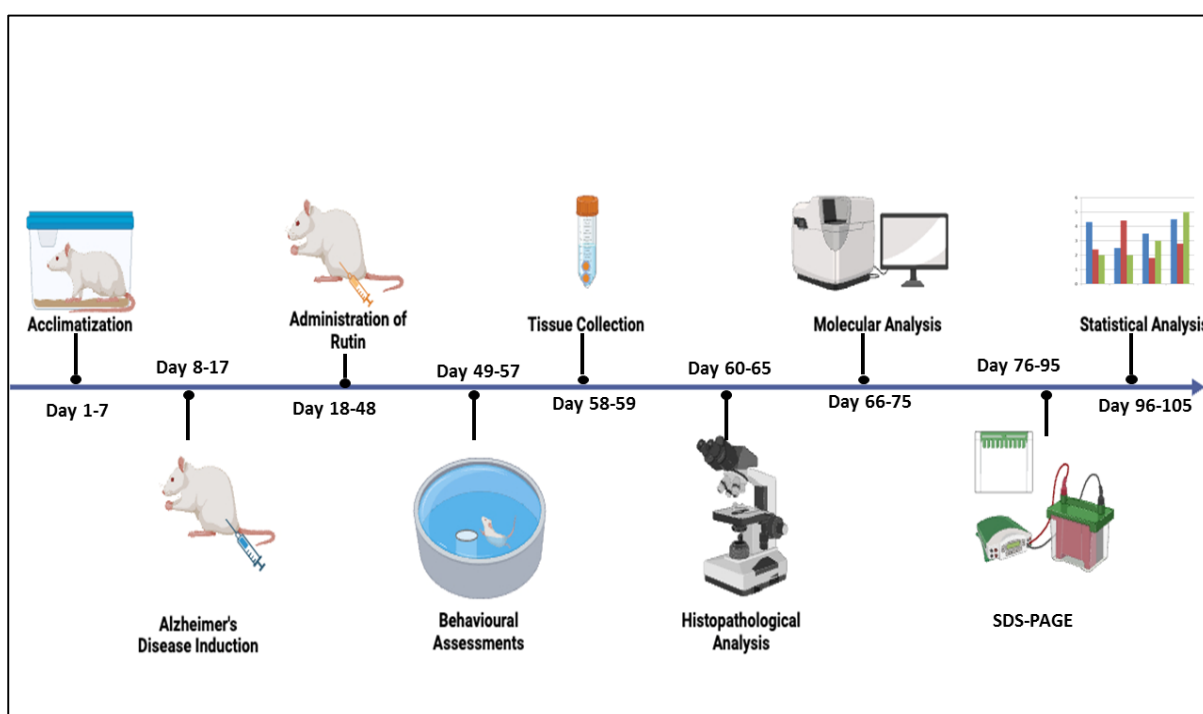
Figure 0.1: **Experimental Design of the Study.** The timeline includes acclimatization and induction of AD, validation of disease, dosages for treatment, behavior testing, dissection and tissue collection, histopathological assessment, molecular and proteomic analysis followed by statistical analysis was applied to validate the results, ensuring the accuracy of data presentation.

2.4. Drug Administration

Three groups of rats were used for drug administration: control, disease, and Rutin treatment. Rutin (207671-50-9, Macklin, China), mixed in DMSO (67-68-5, Sigma Aldrich, Switzerland) was given intraperitoneal to the Rutin treatment group for a month following the induction of AD. Administration of drug was given daily, with dosage adjustments made in accordance with each rat's weight. Rats were constantly watched for any indications of

suffering or negative side effects during the course of the treatment. Rats were dissected when the treatment plan was finished, and brain tissues were taken out for additional examination. The Rutin dosage, 50mg/kg, employed in this investigation was determined based on earlier research (Pu et al., 2007).

2.5. Behavior Testing

Behavioral testing was done after the disease induction and administration of drug to evaluate their cognitive and motor abilities. Morris water maze, Y-maze, open field test, and novel object recognition test were the four behavioral tests used. These assessments were chosen to assess a range of cognitive functions, such as recognition memory, exploratory activity, spontaneous alternation behavior, and spatial learning and memory. Behavioral testing is a crucial component of preclinical research on AD because it provides valuable insights into the pathophysiology of the condition and the efficacy of potential treatment approaches (Webster et al., 2014).

2.5.1. Morris Water Maze MWM test

A cross with the vertices represented the four cardinal points, North (N), South (S), East (E), and West (W), separated the maze into four quadrants. The platform was set in the same location (SW), however the animal was submerged in the water for each trial, beginning in a randomly selected quadrant, that does not contain the platform. The rats had to locate the hidden platform with 10 cm in diameter and submerged 1.5 cm below the water's surface during the five days of acquisition training trials (two trials each day). The rats in each session were allowed to search for the submerged platform for up to ninety seconds, and once they did, they may remain there for ten seconds, as shown in figure 2.2. A maximum score of 90 seconds was given and the training was stopped if a rat was unable to locate the platform in 90 seconds. The escape latency for a single rat's spatial learning score was measured as the amount of time it took to get to the hidden platform. In order to evaluate the spatial memory, a probing test was carried out 24 hours following the acquisition phase by taking the platform out of the tank. For sixty seconds, rats were free to swim. Spatial memory was measured by calculating the percentage of time a single rat spent in the target quadrant that had previously included the platform (Bromley-Brits et al., 2011).
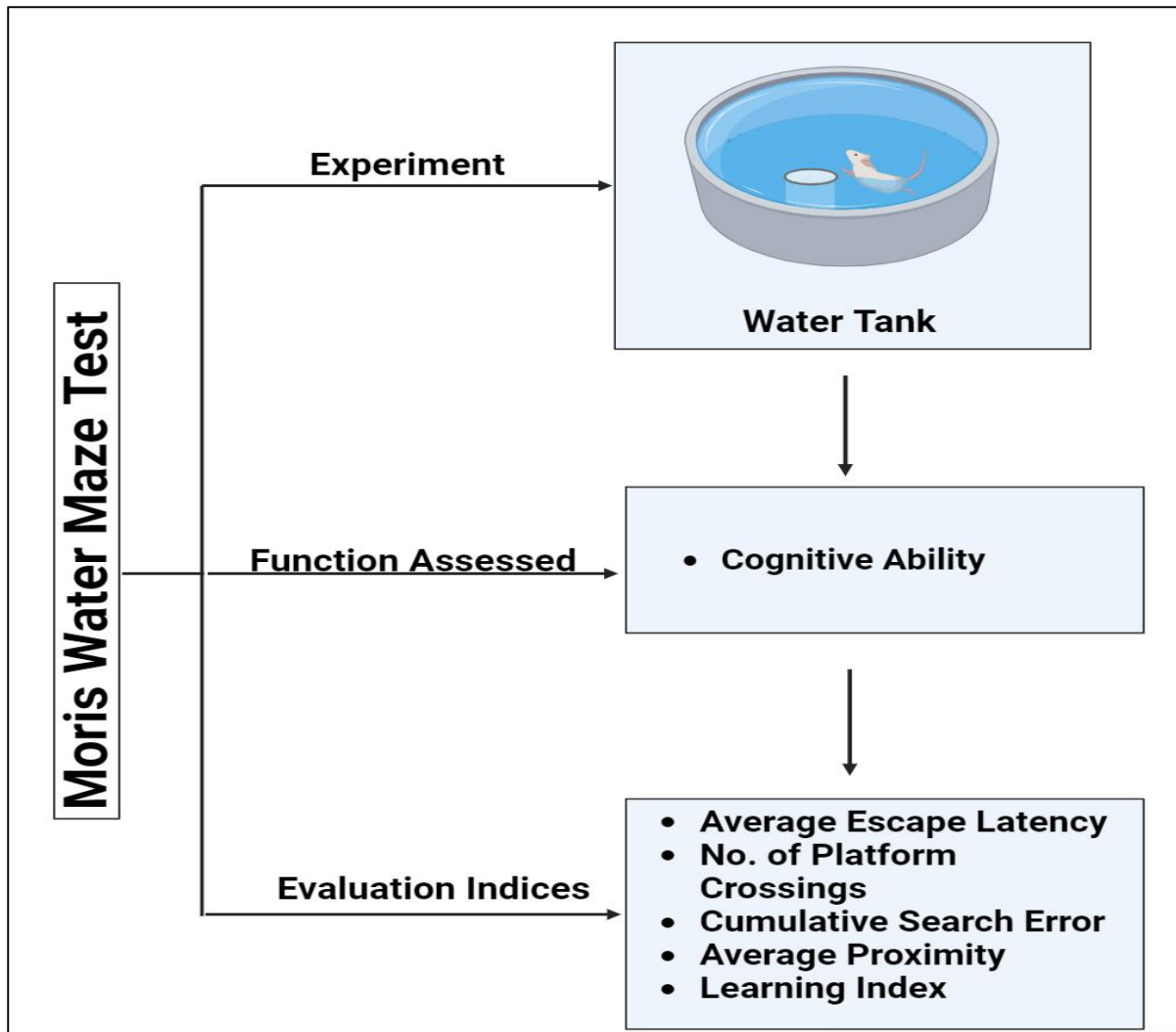
Figure 0.2: Morris Water Maze Test. This test is used to assess the spatial and memory in rodents. Animals are placed in the circular water tank and must find a hidden platform. It provides insights into cognitive function, memory retention, and the effects of neurological conditions or treatments.

2.5.2. *Y-Maze Test*

The foundation of this test is the natural inclination of rat to switch limbs when investigating a novel area., test animals were kept in a Y-shaped labyrinth for five to ten minutes, as shown in figure 2.3. During that time, the number of arms they entered and the order in which they entered were noted, and a score was computed to ascertain the percentage (%) of alternation, degree of arm entries without repetitions. The three arms ($8 \times 30 \times 15$ cm) that made up the Y-maze contraption were spaced $120°$ apart. The Y-maze test included two trials with a one-hour gap between them. The first experiment lasted for ten minutes. Only the first two arms (the familiar and start arms) of the maze were open to the rats' exploration; the third arm (the new arm) was closed off. In the second trial, mice were put back in the starting

arm of the maze and permitted to freely move around all three arms for five minutes (Tolman & Ritchie, 1943).

$$Percentage\ of\ Alteration = \frac{\text{Number of Alterations}}{\text{Total Number of Entries}} \times 100$$

2.5.3. Novel Object Recognition (NOR) Test

Another behavioral evaluation tool that is mostly related to cognitive capacity is the new object recognition test. Three phases make up the novel object recognition test: training, testing, and habituation. Rats were habituated to the arena by spending ten minutes in an empty plastic chamber measuring $15 \times 15 \times 25$cm on the first day, as shown in figure 2.4. The rats were given three minutes to investigate the two objects that were positioned symmetrically along the arena's center line on the second day (training stage). Each object's exploration time was recorded as a gauge of exploratory activity. The third day (testing stage) began with the rodents being put back in their cages for three minutes. One of the objects was moved to a nearby quadrant, and the rats were free to investigate the objects once more. The amount of time spent inspecting and inhaling every item was noted. In order to remove smell cues, the box was washed with 70% alcohol in between experiments (Richler et al., 2017).

2.5.4. Open Field Test

The Open Field Test, one of the most widely used anxiety tests, involves placing mice for ten to fifteen minutes in an empty square or circular arena without a ceiling. The animals were put in a field that was open, and its movements were noted. The wooden box, measuring 60×60 cm with walls 60 cm high, had been used to build the open field apparatus, figure 2-5. Every piece of equipment apart from the white floor was painted black. The floor was divided into sixteen equal-sized squares, each measuring fifteen by fifteen centimeters. For the duration of the experiment, the animals' movements were recorded for five minutes using a video camera that was placed some distance away from the arena. The primary variables that were recorded during the test included the following: rearings, the number of times the animal stands on its hind legs, crossings, the number of times the animal crosses a square with all four legs, latency, the amount of time it takes to leave the beginning square, and grooming the frequency of grooming activities (Hrnkova et al., 2007).
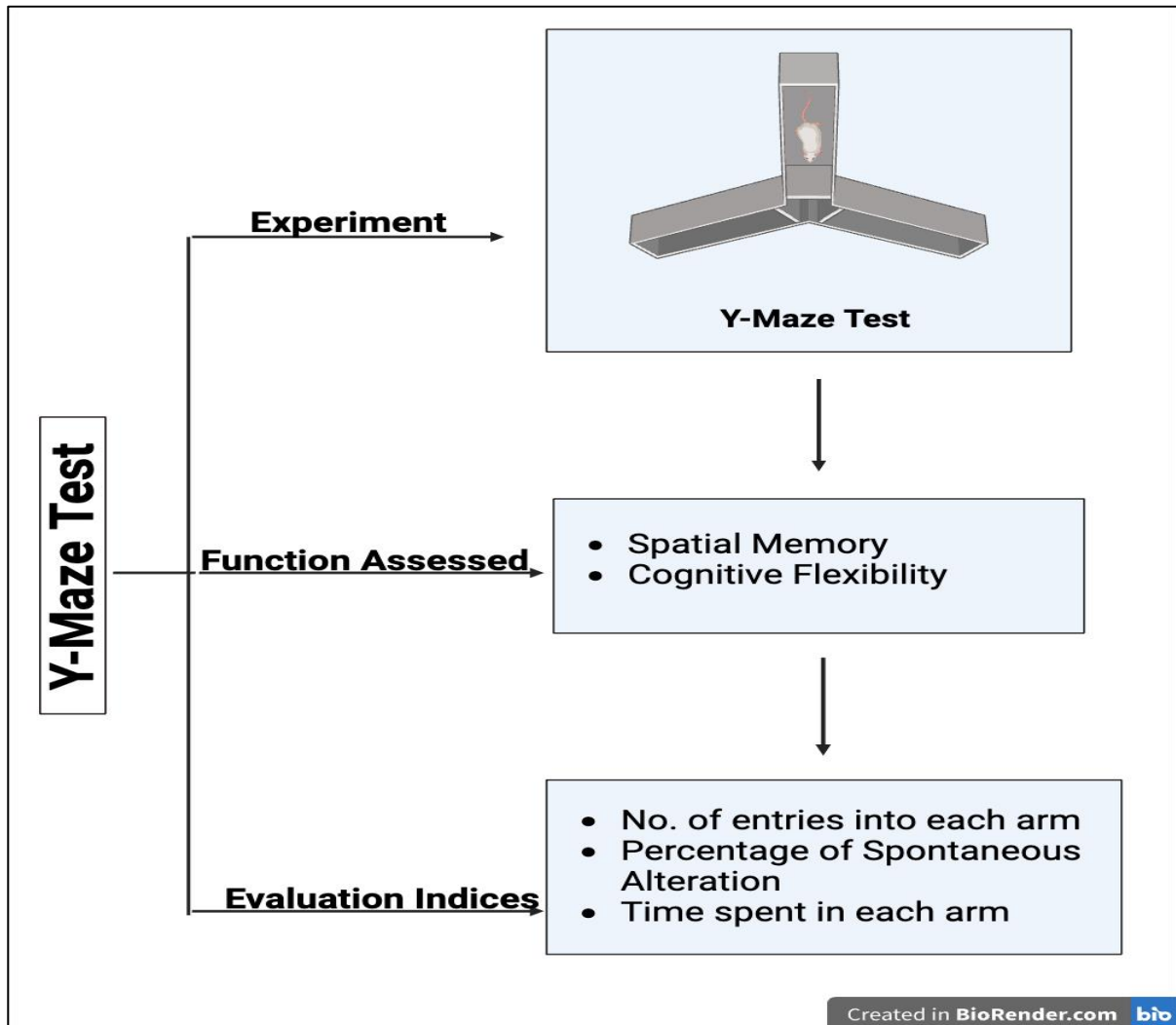
Figure 0.3: Y-Maze Test for spatial memory and exploratory tendency. This figure portrays a rat transitioning from the initial arm to either a familiar arm or a novel arm in the Y-Maze Test. The quantity of time spent in the old and new arms is calculated to determine the percentage of alteration. This percentage is indicative of the rat's spatial memory and exploratory tendencies, providing valuable insights into its cognitive abilities.

2.6.Dissection and Brain Tissue Preparation

All animals were given a profound anesthesia by inhaling chloroform after undergoing behavioral testing. A thoracic incision was made using a trapezoid cut. To provide room for the implantation of a perfusion cannula (23 gauge) into the right ventricle, a little incision was created in the upper left atrium. Normal saline was used for five minutes, followed by a two-to three-minute infusion of 4% PFA in PBS prepared with RNase-free water at a pH of 7.4. To extract the RNA. The brain was extracted and immediately put in a freezer set at -80°C. The skull was then painstakingly dissected and cut in half along the mid-sagittal plane with tiny

scissors, starting at the cerebellum and ending at the bony area encircling the smell bulbs. Each brain was split sagittally into two halves: the left hemisphere was utilized for protein analysis and the right hemisphere for RT-PCR. The cortex was swiftly dissected on ice, snap-frozen, and kept at -80°C for the molecular analysis.
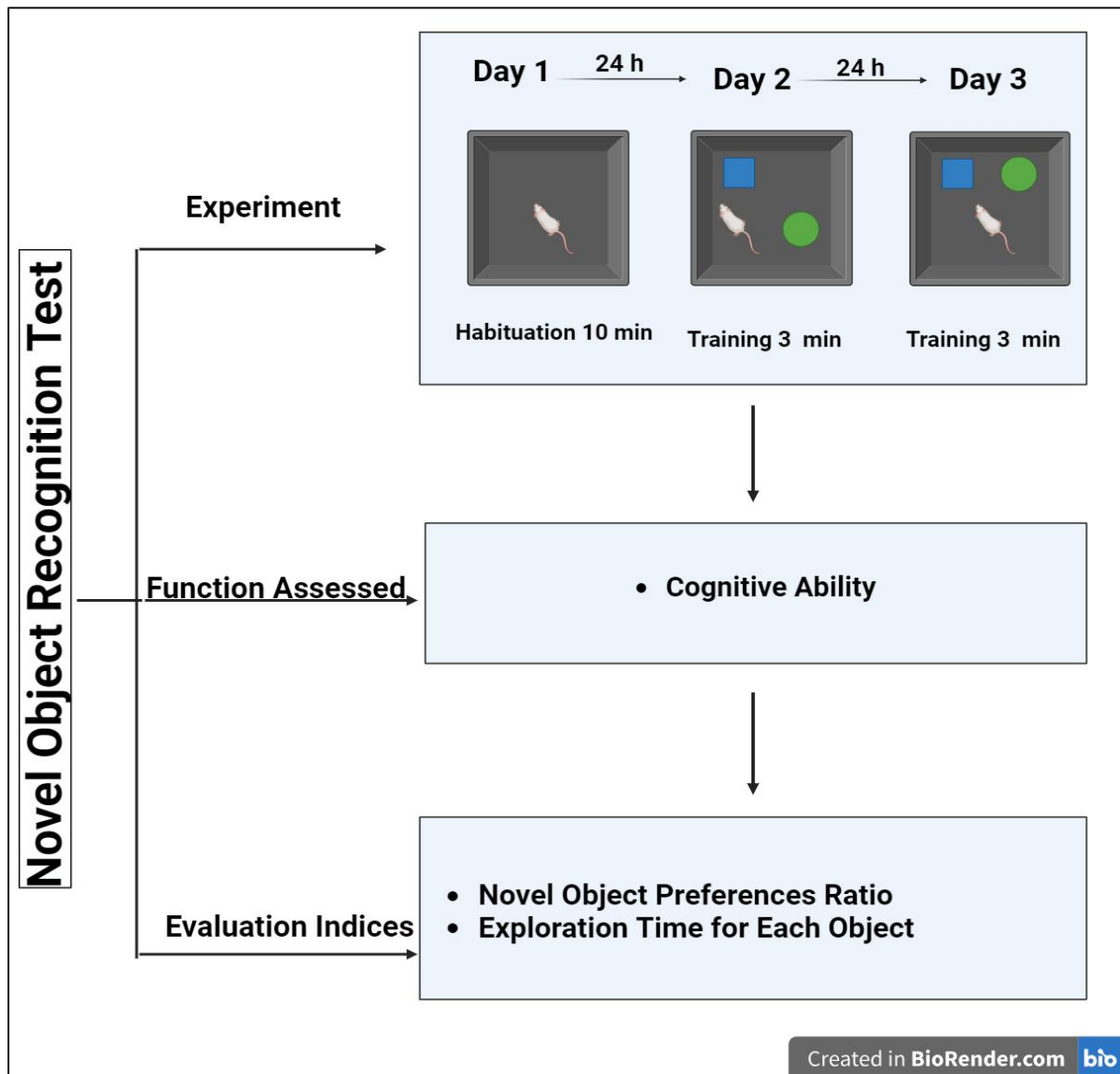
Figure 0.4: Novel Object Recognition Test for cognitive processes. This figure depicts the movement of the rat between the two objects, one familiar and one novel object. It calculates the amount of time spent with each object. The preference for the novel object, as indicated by a greater amount of time spent with it, suggests that the rat remembers the familiar object and perceives the novel object as new. This test is particularly valuable in the field of neuroscience for studying cognitive processes such as memory and attention in rodent models.
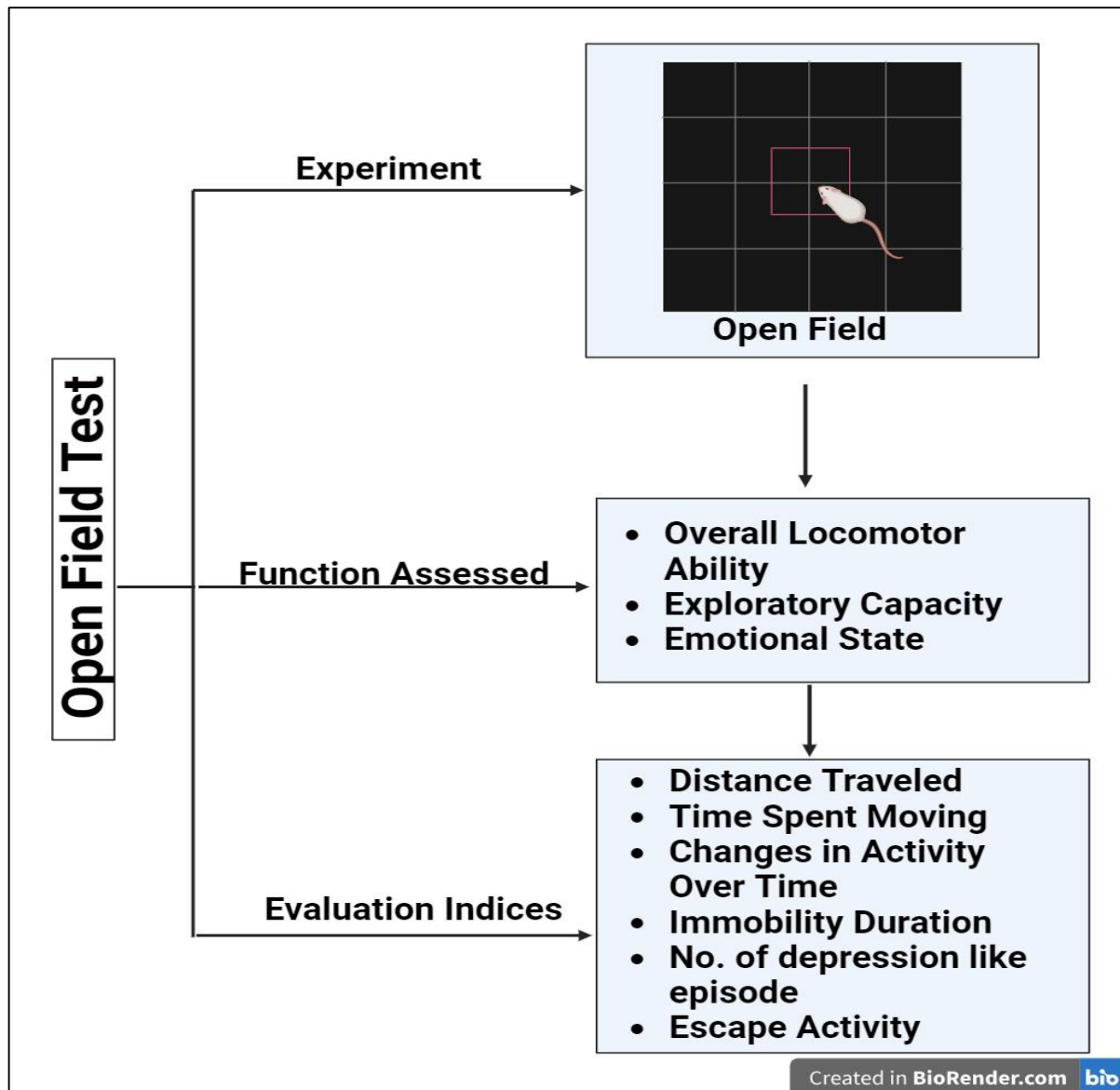
Figure 0.5: Open Field Test for exploratory behavior and anxiety level. This figure shows the movement of the rat across the squares. The time a rat spends in the central region and time spent in peripheral region is calculated. These measurements are crucial as they can provide insights into the rat's exploratory behavior and anxiety levels.

2.7. Histopathological Analysis

The brain was dissected and 4% PFA was passed through left ventricle after saline perfusion to prepare the brain tissue for histological investigation. Complete fixation was achieved by immersing it in 4% PFA for a suitable amount of time, usually between 24 and 48 hours, to enable complete fixation. Different staining techniques are employed to detect specific structures, cells, tissues, or even metal components as the H&E staining is the most widely used method; it shows the nucleus in blue and the cytoplasm of cells in pink, and ThT staining is used to detect accumulation of amyloid plaques.

2.7.1. *Haematoxylin and Eosin Staining (H&E)*

Fixed tissues from one brain of each group i.e., control, diseased and treated were sliced into approximately 4 μm thin slices and microscopic slides were prepared. These slides were deparaffinized by incubating them at 63°C for almost 30 minutes. Additionally, during incubation, slides were submerged in xylol for two minutes before being cleaned with different ethanol concentrations (100%, 90%, 80%, and 70%). Hematoxylin was used for three minutes, followed by a one-minute water wash, a one-minute differentiator with mild acid, another one-minute water wash, bluing, another one-minute water wash, ethanol, eosin, ninety-five percent ethanol, one-minute 100% ethanol, and finally, two minutes of xylene. At the end, slides prepared were covered with a coverslip (Feldman et al., 2014; Alturkistani et al., 2015).

2.7.2. *Thioflavin T Staining*

ThT was prepared by making the working solution of 0.0.5g of ThT dissolved in 0.1 N HCl. The 0.1 N HCl was made by diluting 1.63 ml of concentrated HCl in 200 ml of distilled water. A drop of staining solution was then placed on the slide containing sample and kept in a humidity chamber for 15 minutes to ensure proper staining. After that the slides were rinsed with deionized water for 5 minutes to remove any unbound dye. Finally, the slides were covered with aqua mount cover slip and examined under fluorescent microscope to visualize staining pattern and protein aggregation. The slides were stored in a dark place to maintain integrity of staining.

2.8. Microscopy

A Binocular Light Microscope (S37242, Labo America Inc. USA) for cell count and a fluorescent microscope (1450030, Bio-Rad, USA) for accumulation of Aß, with a 4X–100X magnification, was used to view H&E and ThT slides. Slides were displayed with a 20X magnification. Cells were counted and viewed in the cortex tissues using Image J software, and the differences were compared.

2.9. Analysis of Gene Expression

RNA was extracted from the brain tissue followed by cDNA synthesis for RT-PCR analysis. Gradient PCR was used to optimize primer annealing temperatures before the RT-

PCR studies were carried out. The ideal temperature for a given pair of primers was determined using gradient PCR by evaluating a range of annealing temperatures in many PCR reactions.

2.9.1. RNA Extraction

TRIzol Reagent (FineBiotech Cat. No.: FTR-100, China) was used for the RNA extraction process, which included few steps. Tissue sample with 50-100 mg in weight required the addition of 1 mL of TRIzoL reagent. A power homogenizer was used to completely homogenize the tissue sample. The sample was then incubated at room temperature for 5 minutes, an additional centrifugation step at 12,000 rpm for 10 minutes at 4°C was important for samples containing a high concentration of proteins, polysaccharides, or extracellular material. Subsequently, the supernatant was cleaned and transferred to a fresh tube for further analysis. After that, 0.2 ml of chloroform was added and gave the tube a vigorous 30 second shake, incubated it for 2 to 3 minutes at room temperature and centrifuged it at 4°C for 10 minutes with 12000 rpm. The aqueous phase was pipetted out into a fresh tube and added 0.5 mL of 100% isopropanol. Incubated the supernatant for 10 minutes and centrifuged it for 10 minutes at 4°C. The RNA pellet remained in the tube after the supernatant was removed, as shown in figure 2.6. Ethanol was used to clean the pellet. The sample was vortexed quickly, then the tube was centrifuged at 12000 rpm for few minutes at 4°C. The washer buffer was discarded and allowed RNA pellet to air dry. The RNA pellet was dissolved in 20-50 ml of RNAse-free water and stored it at -80°C till further use.

2.9.2. Assessment of RNA Quality and Quantity

RNA quality and quantity were evaluated using a Nanodrop spectrophotometer prior to cDNA synthesis. The absorbance at 260 nm was used to determine the concentration of RNA, and the ratios of absorbance at 260 nm/280 nm and 260 nm/230 nm were used to assess the purity. High-quality RNA appropriate for use in downstream processes was indicated by optimal ratios. The amount and caliber of the extracted RNA were quantified using Colibri NanoDrop (TitertekBerthold, Germany).

2.9.3. cDNA Synthesis (Reverse transcription)

The RNA extraction was later followed by cDNA transcription with RevertAid Reverse Transcriptase (EP0441, Thermo Fisher Scientific, Lithuania). The reaction mixture was subsequently produced, comprising the reaction buffer, dNTPs, reverse transcriptase, oligodts,

dithiothreitol (DTT), and the RNA sample. The reaction mixture was incubated in the thermal cycler at a particular temperature of 42˚C for 60 minutes

Figure 0.6: **RNA Extraction Through TRIzol Method.** The white pellet at the bottom of the tube shows precipitation of RNA which is now ready for further analysis.

2.9.4. Primer Designing

The primers were selected from the published literature. The primers had the calculated annealing temperature of 66 ˚C for SOD2 and TLR4, as shown in table 2.1. The primers were ordered from Bionics (Islamabad, Pakistan).

1.7.1. Gradient PCR for Primer Optimization

The sample was created using gradient PCR to optimize the primer and estimate the annealing temperature. The conditions of the PCR are very delicate, and they must be fine-tuned to improve the efficient amplification of target genes. In this study gradient PCR was performed in which the annealing temperature was determined for the amplification of SOD2 and TLR4 genes with its specific primer. Gradient PCR profile is as follows. a preliminary denaturation step lasting three minutes at 94°C, 35 cycles lasting thirty seconds at 94°C, and an annealing step lasting thirty seconds at 58 °C to 68°C, as shown in table 2.2. An extension step lasting 45 seconds at 72°C and a final extension lasting 7 minutes at 72°C were then added to the gradient temperatures. The agarose gel electrophoresis method was used to evaluate the purity of the PCR result.

Table 0.1: List of Primers. The table shows the forward and reverse primers of Beta Actin, SOD2, TLR4 with their specific length, sequence and optimized annealing temperature.

Gene	Direction	Length	Sequence (5' to 3')	Annealing Temp (°C)
Beta-actin	Forward	19	CATCCCCCAAAGATTCTAC	57
	Reverse	17	CAAAGCCTTCATACATC	
Superoxide dismutase 2 (SOD2)	Forward	22	CAGACCTGCCTTACGACTATGG	62
	Reverse	21	CTCGGTGGCGTTGAGATTGTT	
Toll-like receptor 4 (TLR4)	Forward	20	GTGGGTCAAGGACCAGAAAA	61.1
	Reverse	19	GAAACTGCCATGTCTGAGCA	

Table 0.2: Gradient Temperatures for Primer Optimization. The table displays the range of annealing temperatures used for gradient PCR

Gradient Temperature °C					
58°C	60°C	62°C	64°C	66°C	68°C

2.9.5. Reaction Mixture

The PCR tube was filled to a total capacity of 25µl with 12.5µl of PCR master mix (Wizbio Solutions, catalog no: W1401-2, South Korea), 8.5µl of Nuclease-free water, 1µl of forward primer, 1µl of reverse primer, and 2µl of cDNA template.

Table 0.3: List of PCR Ingredients. The table shows the components along with their quantities to make final volume of 25µl.

Sr.No	Products	Quantity (µl)
1	PCR Master mix	12.5
2	Nuclease free water	8.5
3	Forward primer	1.0
4	Reverse primer	1.0
5	cDNA template	2.0

2.9.6. Agarose Gel Electrophoresis

After the completion of the PCR cycles, 5 µL of each PCR result was mixed with a loading dye and placed onto a 2% agarose gel that had been stained with ethidium bromide

(Sigma Aldrich, catalog no. 39346, USA). The gel was run in TBE buffer (catalog no. T1051, Solarbio, China) at 100V for around 30 minutes. The locations of the bands were compared to the 100–1500 bp DNA ladder to see if annealing had taken place. A Benchtop 2UV transilluminator (LM-20 | P/N 95044902, UVP Co., USA) was then used to evaluate the gels. The annealing temperature was one of the cycling parameters of each primer pair that was estimated using gradient PCR data. The ideal temperature for PCR operations was thought to be one that produced a single, crisp band with the least amount of background noise, non-specific amplification, and primer-dimer formation.

2.9.7. Real-time PCR

The expression levels of SOD2 and TLR4 in brain tissues were measured using RT-PCR. The CT-values was used to determine the dysregulated reference gene in AD patients. In every PCR cycle, the fluorescence spectra were captured during the elongation stage. During the PCR exponential phase, the amplification plots and CT-values were exported into a Microsoft Excel worksheet for further analysis. The reaction mixture was prepared using WizPure™ qPCR Master Mix (SYBR Green, Catalogue No: W2631, Wizbio, Korea). The PCR reaction mix is described in table 2.4. The amplification curves employed the quality of the PCR product. The values obtained from these trials were analyzed about gene expression using their ΔCt values after all values were normalized to those obtained for ß-actin.

Table 0.4: qPCR Master Mix Preparation. The table shows the components of qPCR master mix preparation along with their quantities to make 20µl of PCR mix.

Sr.No	RT-PCR Products	Quantity
1.	cDNA template	1.0
2.	Forward primer	1.0
3.	Reverse primer	1.0
4.	SYBR green master mix	4.0
5.	Nuclease free water	13.0
	Total reaction volume	20µl

2.9.8. Cycling Parameters for Real-time PCR

In PCR cycling profile, 35 cycles were employed to achieve targeted DNA amplification. The process begins with a denaturation at 94°C (3 min), followed by annealing

at 66°C (30 s) for SOD2 and TLR4, and last is the elongation at 72°C (45 s), as shown in figure 2.7.
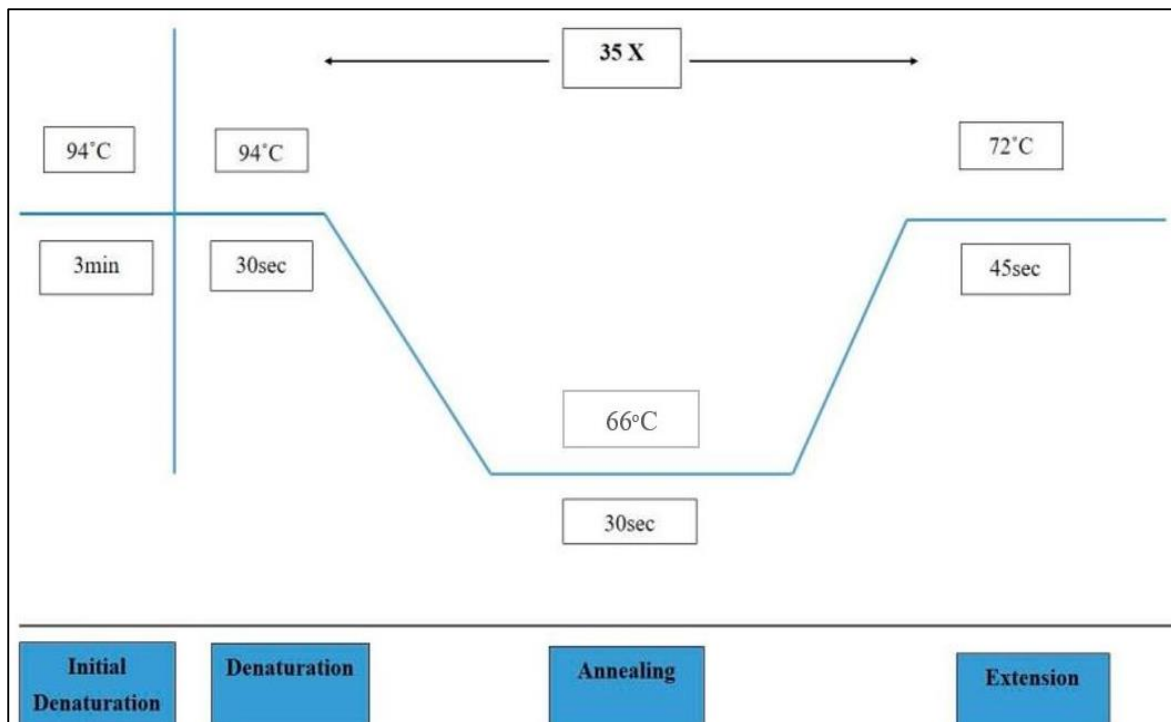
Figure 0.7: Cycling Parameters for qPCR. The figure shows the thermal cycling profile for SOD2 and TLR4

2.10. SDS-PAGE

Electrophoresis is one method for separating macromolecules in an electric field. SDS-PAGE uses sodium dodecyl sulfate (SDS) as the support medium in a polyacrylamide gel to denature the proteins and make them linear. The most popular method is known as the Laemmli method, named for U.K. Laemmli, who published the first SDS-PAGE scientific investigation (Holman et al., 2013). Protein separation using SDS-PAGE can be used to assess protein distribution among fractions, relative molecular mass of proteins, relative quantity of proteins in a sample, and purity of protein samples.

2.10.1. Protocol

2.10.1.1. Sample Preparation

We prepared the sample by weighing 20 mg of brain tissue and 1 ml of SDS lysis buffer (Appendix A) was added to fully submerge the tissue. The sample was then sonicated at 50 Hz for 30 minutes, after that a short spin was performed to remove any forth. The homogenized

sample was placed at 4°C overnight to ensure complete extraction. The following day, centrifugation was performed at 14000 rpm for 30 minutes at 4°C. After centrifugation, supernatant was collected, which contained extracted proteins, without disrupting the pellet. Protein lysates were store at -80°C till further use. Isolates having 50µg tissue protein were taken and distilled water was added respectively in protein isolates and laemmli buffer (Appendix A) was added in each sample. The samples were subjected to 95°C for 5 minutes for thermal digestion. They can be stored at -20°C until use.

2.10.1.2.   Gel Casting

After preparing the protein lysates, gel casting was performed for SDS-PAGE. For that, 12% resolving and stacking gel was made through pre-prepared stock solutions of acrylamide, SDS, tris-HCl and ammonium persulphate (Appendix A). the resolving gel was first prepared by combining these stock solutions along with TEMED to initiate polymerization. The gel solution was poured between glass plates in gel casting apparatus and isopropanol was added on top of resolving gel solution to ensure a smooth surface. After polymerization of resolving gel, isopropanol was removed carefully and stacking gel solution was poured on top of resolving gel and a comb was inserted to form wells for loading of protein samples. After complete polymerization of stacking gel, the gels were ready for electrophoresis.

2.10.1.3.   Electrophoresis

1X running buffer (Appendix A) was prepared by diluting 10X running buffer. The prepared samples were poured into the stacking gel's wells together with a protein marker as reference. The gels were then subjected to electrophoresis tank filled with running buffer at constant voltage 100V till the loading reaches bottom of the gel, approximately 2.5 hours.

2.10.1.4.   Coomassie Staining and Destaining

Once the electrophoresis was done, the gels were removed from the tank and washed with distilled water twice. The gels were fixed in a fixative solution (Appendix A) for one hour. After fixation, the gels were stained with Coomassie Brilliant Blue (Appendix A) for protein visualization and then destained, to remove any excess dye and enhance the contrast of the protein bands against a clear background, overnight with destaining solution (Appendix A). Utilizing Image J software, the destained gels were scanned and examined to measure the protein band intensity, facilitating cross-sample comparisons.
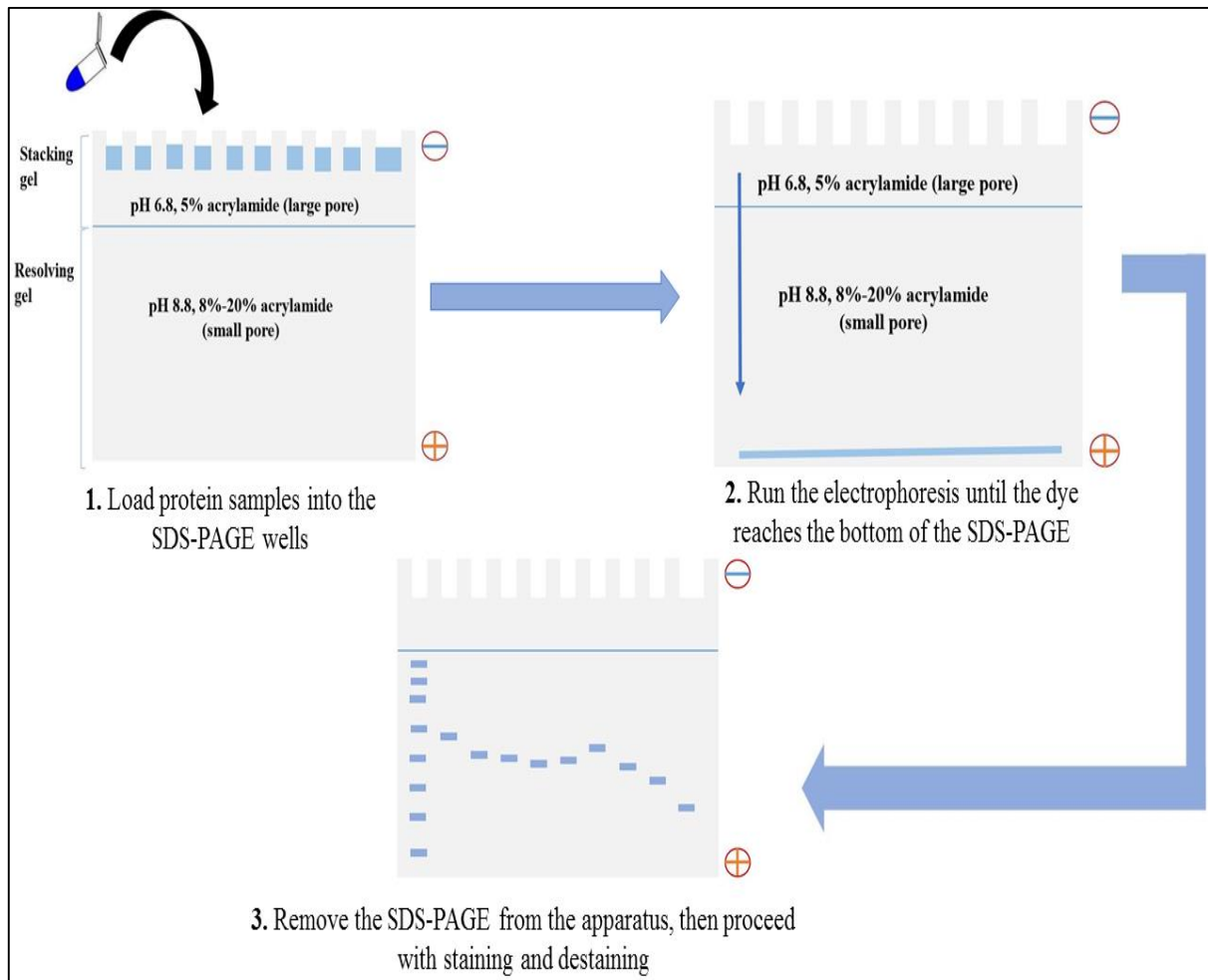
Figure 0.8: Protein separation using SDS-PAGE technique. This figure illuatrates the process of pouring sample into wells of the gel. The bands migrate from negative to positive electrode, which allows for the separation of proteins based on their molecular weight.

3.1.Behavior Assessment Results

3.1.1. Evaluation of Learning and Memory Acquisition

The Morris Water Maze (MWM) test measures an animal's time to escape, frequency of use of the target quadrant, and amount of time spent in the target quadrant to evaluate its spatial learning and recall. Figure 3-1 shows that the control group learned the most about the area with the most entries, the least escape delay, and the longest duration in the target quadrant. In contrast, the diseased group displayed notably longer escape latencies along with less entries and times in the target quadrant, indicating that the CNS disease had a major effect on the learning and retention of spatial memory in these animals. According to the MWM test results, NCDs-Rutin has more of an impact as seen by reduced escape latency, increased entry into the target quadrant, and duration spent there that is comparable to that of the control group. Though not as much as with the NCDs Rutin, both the CDs Rutin treated group and the Rutin therapy group showed improvement.
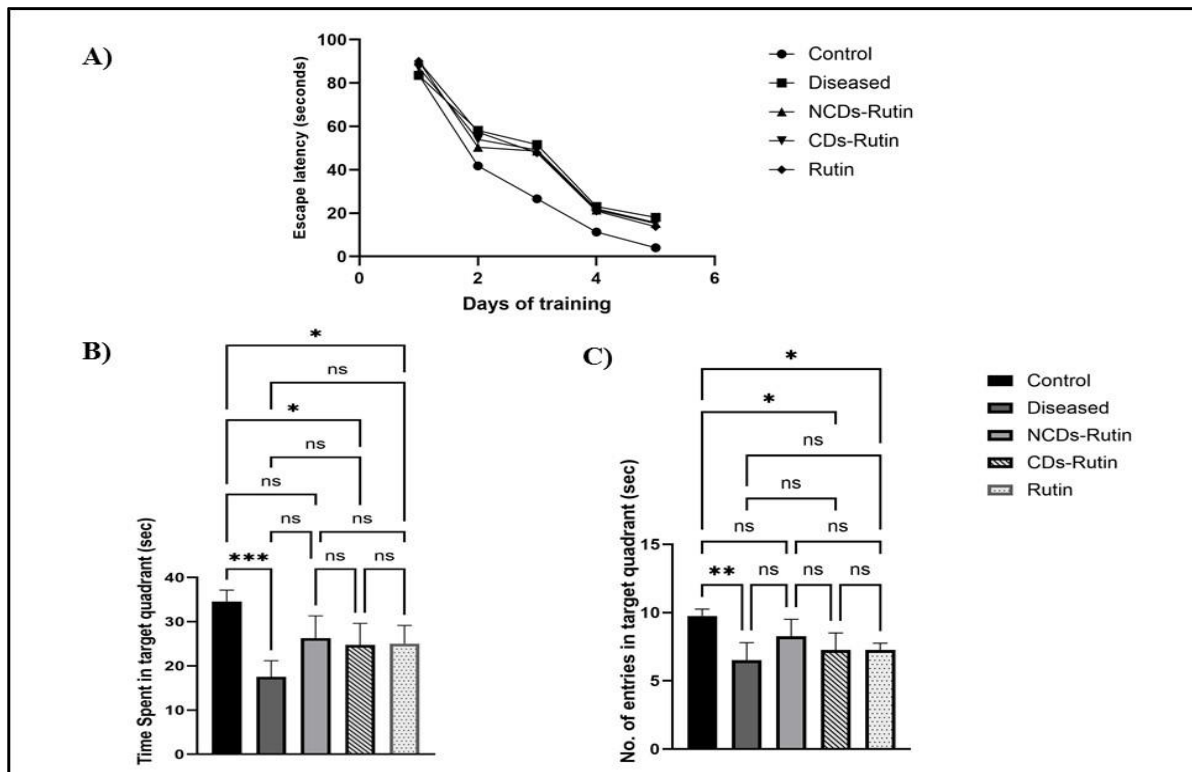
Figure 0.1: Morris Water Maze test results. The graphs illustrate the (A) escape latency over six days of training, (B) time spent in the target quadrant, and (C) number of entries in the target quadrant. One-way ANOVA, followed by Tukey's multiple comparison test, was used for statistical analysis. Error bars present SEM, 'ns' represent non-significant while *, ** and *** represents $p<0.05$, $p<0.01$ and $p<0.001$.

3.1.2. Spatial Memory and Exploratory Tendencies in Y-Maze Test

Five groups were analyzed: control, disease, and three treatment groups, NCDs-Rutin, CDs Rutin, and Rutin. The number of entries in the familiar arm and the novel arm, as well as the percentage of alternations, were also examined in figure 3-2. Based on how many times a rat enters or exits the arms and how much time they spend in each arm, the Y maze test assesses their spatial memory and cognitive ability. In this study, there was a discernible difference in the responses between the diseased and control groups; the control group had more entries in the target quadrant than the diseased group, indicating improved spatial learning and exploratory activity. In line with decreased cognitive ability linked to the AD like state, the diseased group decreased the number of entries and the length of time spent in the target quadrant. However, among the treatment groups, entries of NCDs-Rutin group in novel arm was more than other two treatment groups.
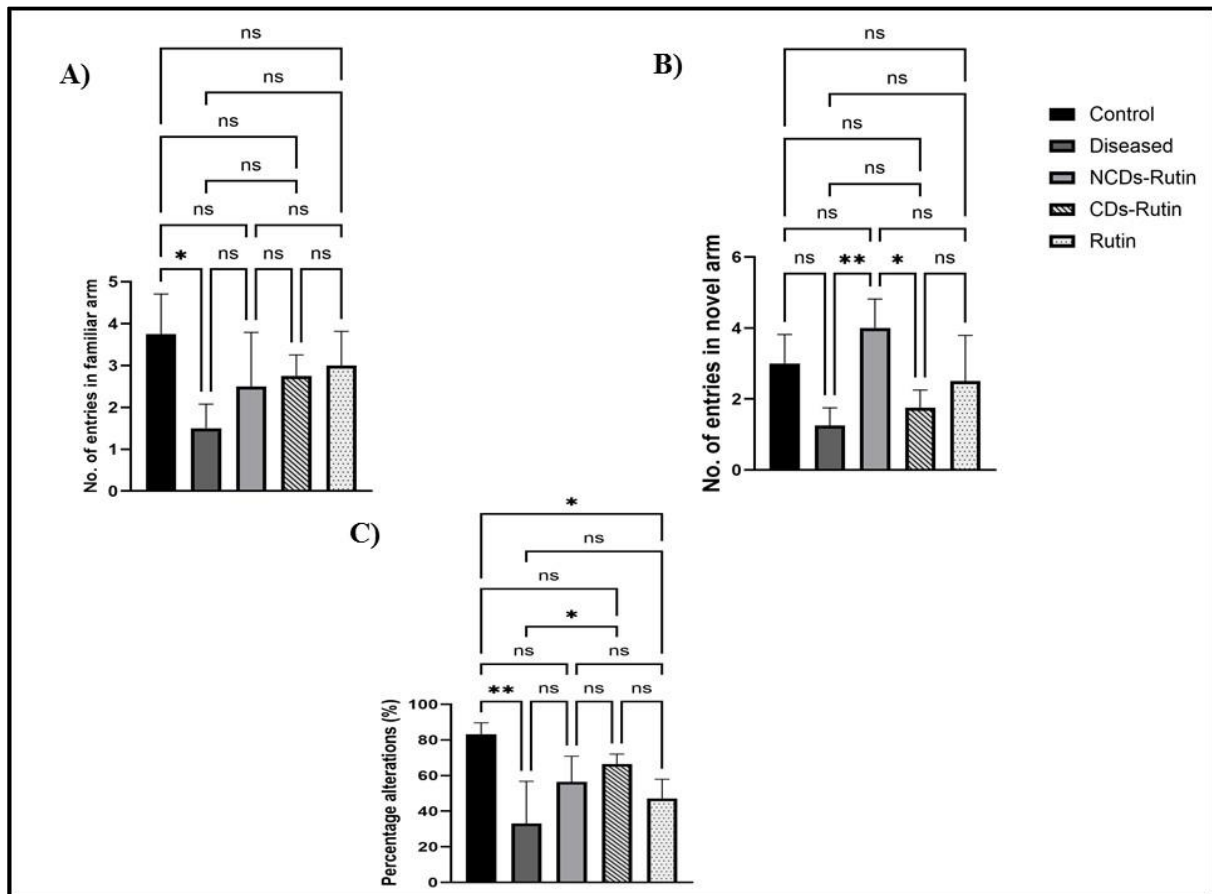
Figure 0.2: Effects of treatments on cognitive function and exploratory behavior in the Y-maze test. (A) Number of entries in the familiar arm across five groups: Control, Diseased, NCDs-Rutin, CDs-Rutin, and Rutin (B) Number of entries in the novel arm. (C) Percentage of alternations, reflecting working memory. Statistical significance was determined using one-way ANOVA followed by Tukey's multiple comparison test with 'ns' represent non-significant while * and ** represents $p < 0.05$ and $p < 0.01$ indicating levels of significance. Data are presented as mean ± SEM.

3.1.3. Evaluation of Exploratory and Anxiety Response

The results of OFT are given in figures 3-3 which shows the duration of stay in CA and PA in various groups of rats. The open field test was conducted to evaluate the anxiety-like behavior. Disease group spent less time in central as compared to control group, while among treatment groups, NCDs-Rutin spent more time in central area. When compared to the disease group, the treatment groups showed an improvement in the amount of time spent in the CA. With averages getting close to 7 seconds, the NCDs-Rutin and CDs-Rutin groups among them demonstrated the most substantial improvements, albeit they were still below the levels of the control group. This implies that these medications may have some anxiolytic impact. Among all the treatment groups, the Rutin group was the least successful, yet it still showed improvement. The diseased group spent the most time in the peripheral area (PA), suggesting higher levels of worry. In line with their enhanced CA performance, the therapy groups spent less time in the PA than the sick group. Nonetheless, there was no discernible difference between the treatment groups' amounts of time spent in the PA. These findings suggest that although various therapies reduced anxiety-like symptoms brought on by AD, none completely brought behavior back to normal levels.
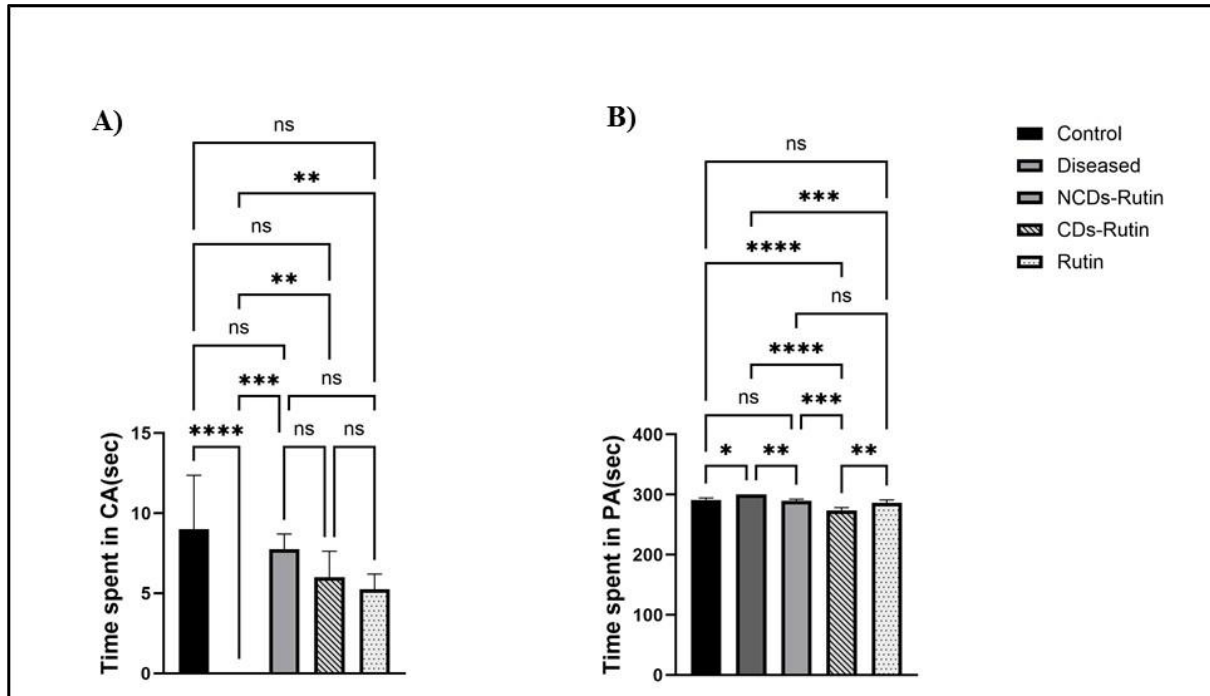
Figure 0.3: Open Field Test Results. The Effects of Alzheimer's disease induction and subsequent treatments on rats' behavior in the open field test. The graphs illustrate the (A) time spent in the center area (CA) and (B) peripheral area (PA) across five groups. Statistical significance was analyzed using one-way ANOVA followed by Tukey's multiple comparison test. Data are presented as mean ± SEM, 'ns' represent non-significant while *, **, *** and **** represents $p<0.05$, $p<0.01$, $p<0.001$, and $p<0.0001$.

3.1.4. Memory Retention and Object Recognition Performance in NOR Test

Rats' cognitive abilities were evaluated using the novel object recognition (NOR) test. The test claimed to measure the amount of time the animals focused on a novel object, a measure that is utilized to assess an animal's potential for memory and recognition. The control group spent 15 seconds to recognize new object, indicating that they had the most intact cognitive function. The disease group, however, showed less time to explore because their investigation time was cut down to only five seconds, which is obviously indicative of cognitive impairment. Positive increases in the exploration time were observed when comparing the outcomes of the therapy groups to the sick group. In the treatment groups, CDs-Rutin group showed the progress in the investigated time. Improvements were also observed in the NCDs-Rutin and Rutin groups during the experiment.
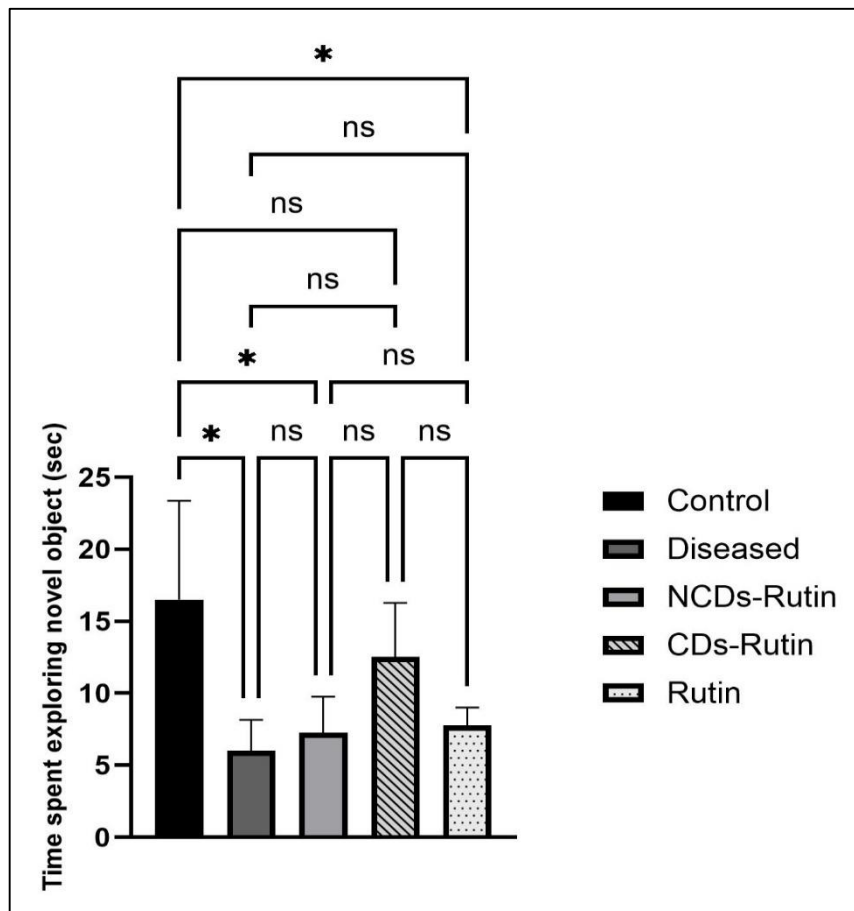
Figure 0.4: Novel Object Recognition Test. The graph represents the control, diseased and treatment groups. The statistical analysis employed for the study involved the utilization of both one-way ANOVA and Tukey's multiple comparison test. The error bars depicted the standard error of the mean (SEM), 'ns' represent non-significant while * represents $p < 0.05$

3.2. Histological Evaluation of Neurodegeneration Changes in AD

Histopathological analyses are crucial to the investigation of AD because they reveal changes in brain tissues at the specific tissue characteristics. The present research provides insights on the neuronal integrity and morphology of the cells, as well as the existence of several pathological characteristics such as neurofibrillary tangles and amyloid-β plaques, which are indicative of AD. Chromotographic methods for total cell density and anatomical brain concerns such as the cortex and the proportionate loss or degeneration pattern of neurons, such as H&E staining.

In the past, thioflavin T (ThT) staining was emploid which binds to amyloid-beta plaques selectively and can be used as a semi-quantitative index of plaque burden as well as to measure the amount of amyloid deposition. Thus, it can evaluate the reversal for neuronal loss and amyloid deposition in this AD model by comparing the histological outcomes between control, diseases, and treatment alternatives such as NCDs-Rutin, CDs-Rutin, and Rutin. This evaluation is crucial because it provides evidence of the efficacy of the treatments by tracking the alterations in cellular and molecular mechanisms brought about by the therapy and comparing them to behavioral changes.

3.2.1. Prevention of neuronal loss

Staining tissues with H&E is a common method in histology for analyzing their morphology and structure. In this study, H&E staining was performed to assess neuronal density and overall cellular integrity in the cortex of AD induced and treatment groups. Hematoxylin stains cell nuclei a deep blue-purple, allowing for clear visualization of nuclear structures, while Eosin stains the cytoplasm and extracellular matrix pink, providing contrast that highlights the overall tissue architecture. In the context of AD, H&E staining is particularly useful for detecting neuronal loss, a hallmark of the disease. The diseased group typically shows a significant reduction in the number of neurons, indicative of neurodegeneration.

In the control group, a high density of neurons with well-preserved cell morphology was observed, indicating healthy and intact cortical tissue. Conversely, the diseased group, representing AD induction, showed a significant reduction in neuronal density. The neurons appeared more dispersed with signs of degeneration, reflecting the neurodegenerative impact of Alzheimer's. Treatment with NCDs-Rutin showed a marked improvement in neuronal density compared to the diseased group. The tissue integrity appeared better preserved,

indicating a neuroprotective effect. Similarly, the Rutin treatment group displayed an improvement in neuronal density over the diseased group. While the neurons were more densely packed than in the diseased group, the overall density was lower than in the NCDs-Rutin group. These results suggest that both NCDs-Rutin and Rutin treatments have neuroprotective effects, with NCDs-Rutin showing a potentially greater impact on preserving neuronal density in the cortex. The visual inspection supports these findings, indicating improvement in cellular integrity and reduction in neurodegeneration markers in the treatment groups compared to the diseased group, as shown in figure 3.5.
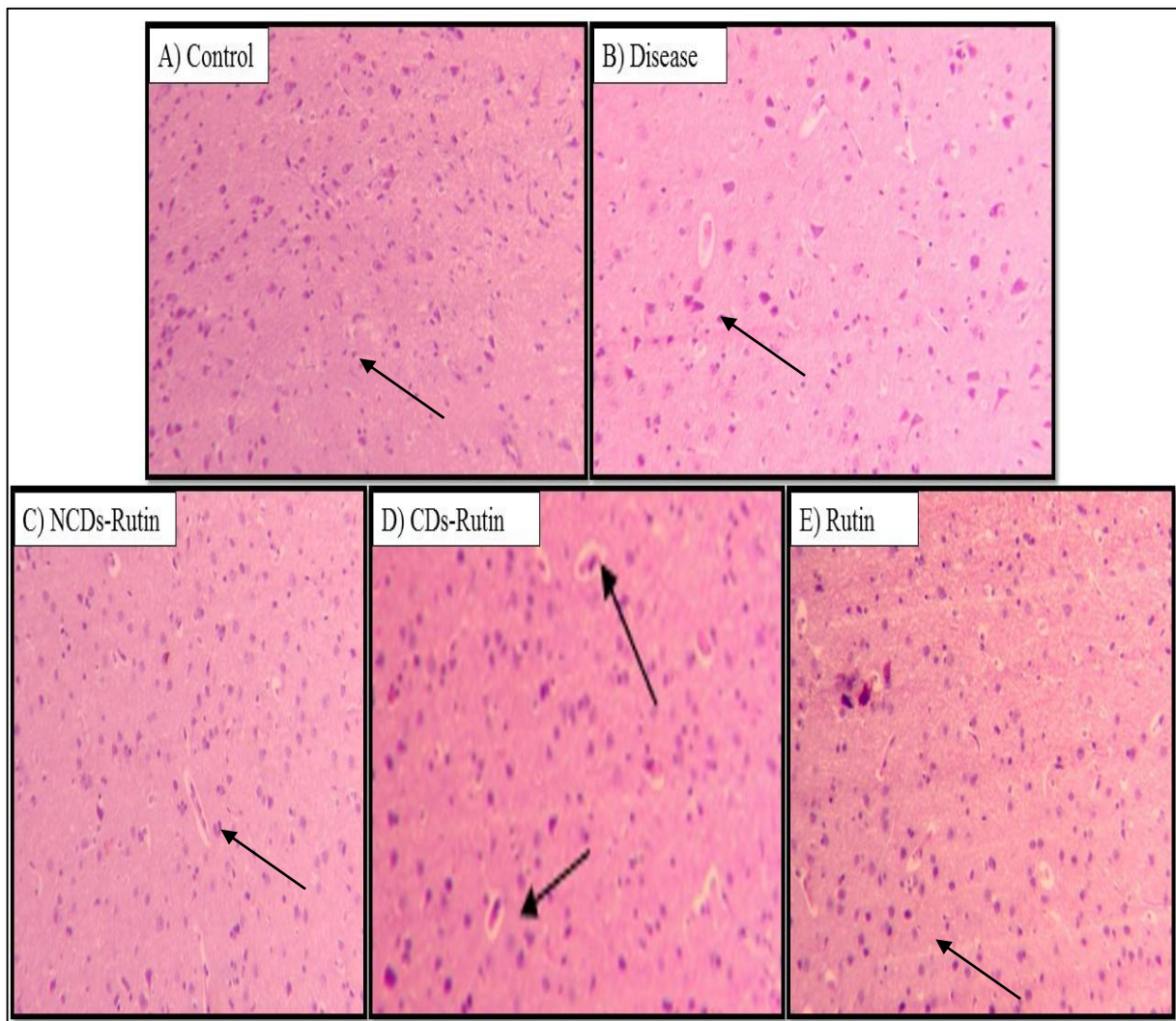
Figure 0.5: **Histological examination of the cortex using H&E staining.** Representative micrographs show the neuronal cell density in the cortex across different groups. (A) Control group, (B) Diseased group (Alzheimer's model), (C) NCDs-Rutin treated group, (D) CDs-Rutin, and (E) Rutin treated group.

3.2.1.1. Neuronal Density in Cortical Region

The control group exhibited the highest number of cortical neurons, with a mean count exceeding 4000, reflecting healthy, undamaged tissue. In contrast, the diseased group,

representing AD induction, showed a significant reduction in neuronal count, with a mean around 2000, indicating substantial neurodegeneration typical of Alzheimer's pathology. Treatment with NCDs-Rutin demonstrated a significant improvement in neuronal density compared to the diseased group, with a mean count approximately 3000. This result suggests a neuroprotective effect of NCDs-Rutin, as evidenced by the significant differences ($p<0.001$) when compared to the diseased group. Similarly, the CDs-Rutin and Rutin groups also showed significant increases in neuronal density compared to the diseased group, albeit to a slightly lesser extent than NCDs-Rutin. Both groups had mean neuronal counts closer to 2500, highlighting their beneficial impact on cortical neuronal preservation.

Despite the improvements seen with all three treatment groups, there were no statistically significant differences among them, suggesting that while each treatment offers neuroprotection, their efficacies are comparable. The significant differences observed between the control and diseased groups underscore the extent of neuronal loss due to Alzheimer's, while the treatment groups' improved neuronal counts illustrate their potential in mitigating such neurodegeneration. These findings support the therapeutic potential of Rutin and its nanoparticle-bound forms in preserving neuronal integrity in AD models.

3.2.2. *Analysis of Amyloid Aggregation with Th T Staining*

The ThT staining results, as shown in image 3.7, highlight the presence and distribution of amyloid plaques in the cortex of different experimental groups, shown in figure 3.7. Image A depicts the control group, showing a sparse distribution of amyloid plaques, as expected in healthy brain tissue. Image B, representing the disease control group, shows a marked increase in amyloid plaque accumulation, indicating successful induction of AD pathology. This serves as a baseline to compare the effectiveness of the treatment groups. In Image C, the NCDs-Rutin treated group demonstrates a noticeable reduction in amyloid plaques compared to the disease control group. This suggests that the combination of NCDs and Rutin has a beneficial effect in mitigating amyloid deposition. Image D shows the CDs-Rutin treated group, which also exhibits a reduction in plaque accumulation, albeit slightly less pronounced than the NCDs-Rutin group. This indicates that CDs in combination with Rutin are effective but potentially less so than NCDs. Finally, Image E shows the group treated with Rutin alone. This group also

shows a reduction in amyloid plaques compared to the disease control group, though the reduction appears to be less significant compared to the other two treatment groups.
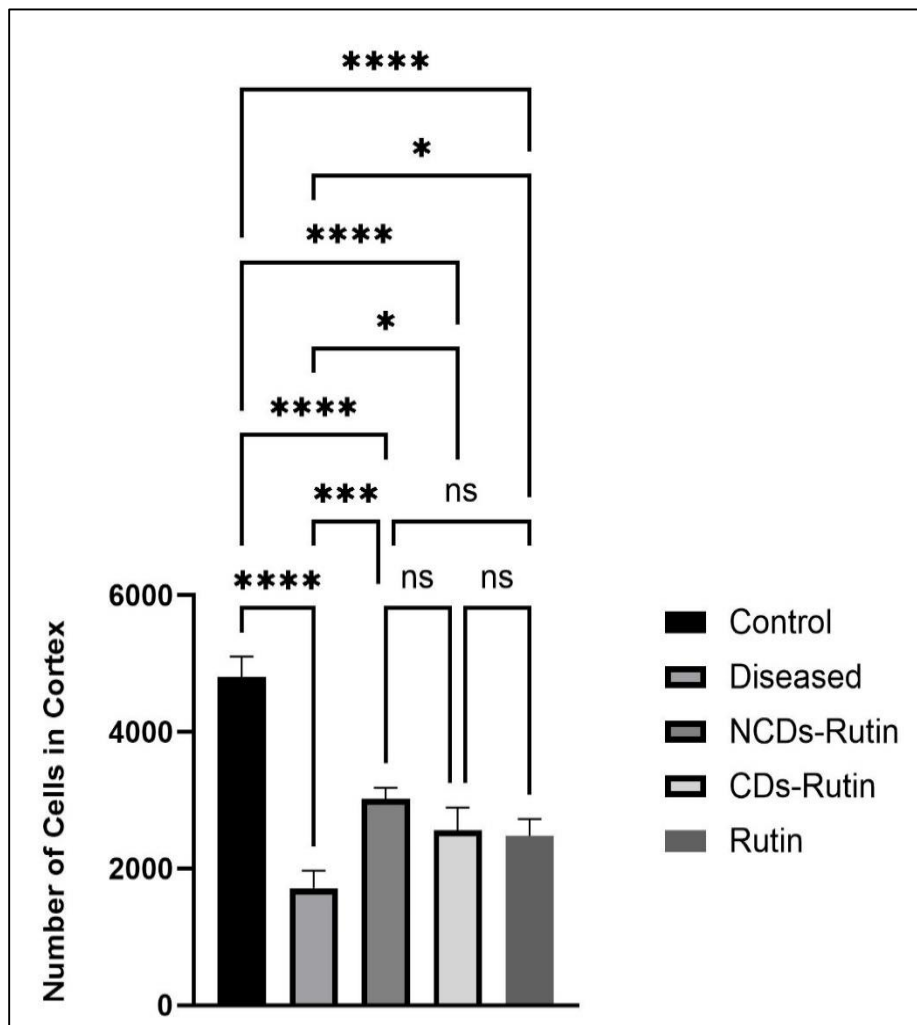
Figure 0.6: Quantification of neuronal cell count in the cortex using H&E staining. The graph compares the number of cortical neurons across five groups: Control, Diseased, NCDs-Rutin, CDs-Rutin, and Rutin. One-way ANOVA, followed by Tukey's multiple comparison test, was used for statistical analysis. Error bars present SEM, 'ns' represent non-significant while *, *** and **** represents $p < 0.05$, $p < 0.001$, and $p < 0.0001$.

3.2.2.1. Limited Formation of Aβ Aggregates

The ThT staining results, figure 3.8, illustrate the impact of AD and the subsequent effects of various treatments on amyloid plaque accumulation in the cortex. The control group exhibited the lowest number of amyloid plaques, highlighting a baseline condition with minimal pathological changes. In stark contrast, the disease control group showed a significant increase in amyloid plaque accumulation, a hallmark of AD pathology. This increase was statistically significant (**** represents $p < 0.0001$) compared to the control, figure 3.8, confirming the successful induction of the disease model. Treatment with NCDs-Rutin, CDs-

Rutin, and Rutin demonstrated a notable reduction in the number of amyloid plaques compared to the disease control group, indicating the therapeutic potential of these treatments. The NCDs-Rutin group showed a significant reduction (* represents $p < 0.001$) in amyloid plaques. However, no significant differences were observed among the treatment groups themselves (ns, not significant), suggesting comparable efficacy in reducing amyloid plaque burden.
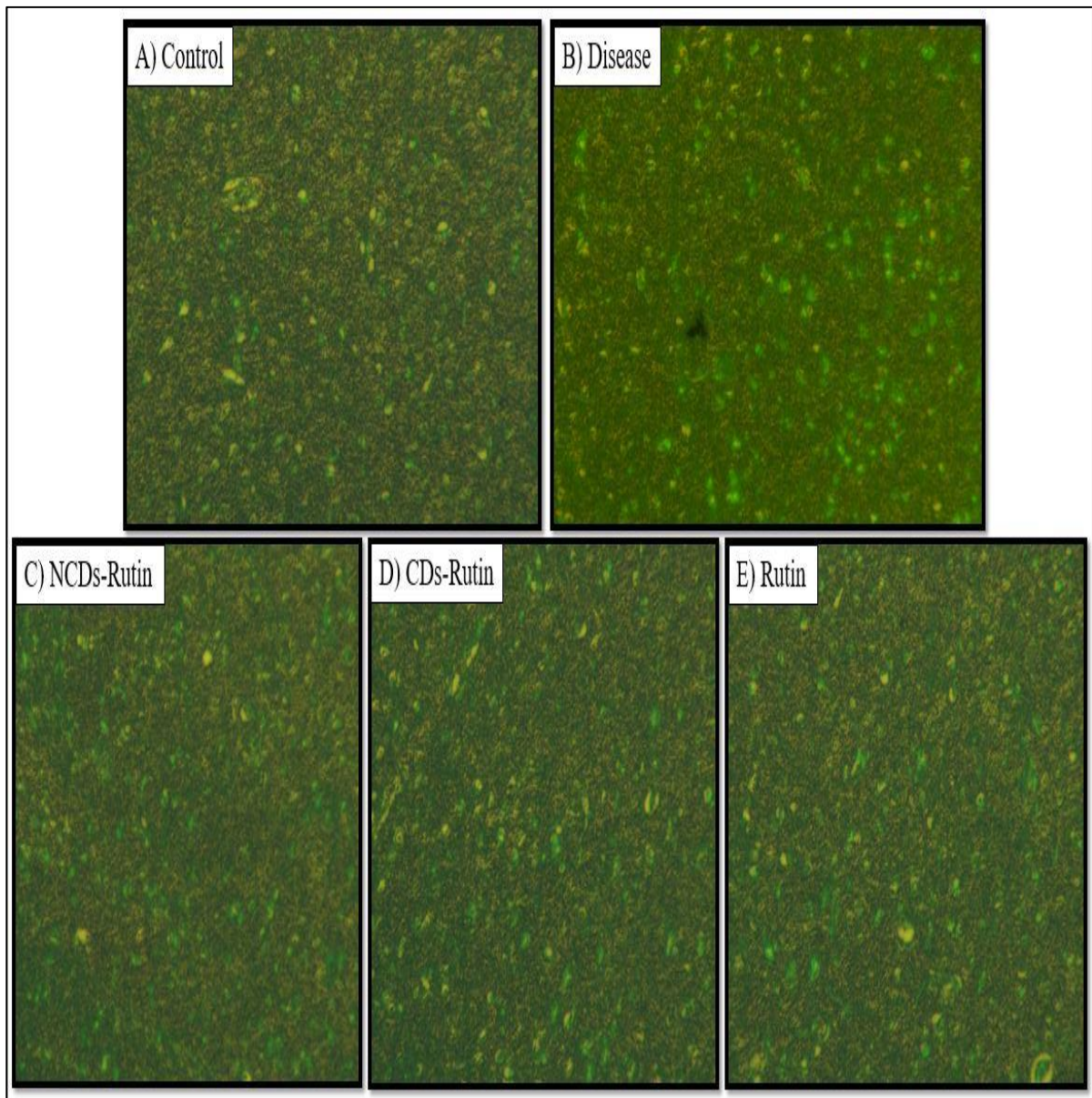
Figure 0.7: Thioflavin T (ThT) staining results of amyloid plaque distribution in the cortex across different experimental groups. (A) Control group, showing minimal amyloid plaque accumulation. (B) Disease control group, showing significant amyloid plaque accumulation. (C) NCDs-Rutin treated group, demonstrating a reduction in amyloid plaques. (D) CDs-Rutin treated group, showing a reduction in amyloid plaques, less pronounced than the NCDs-Rutin group. (E) Rutin treated group, showing a reduction in amyloid plaques compared to the disease control group, but less significant than the NCDs-Rutin and CDs-Rutin groups.
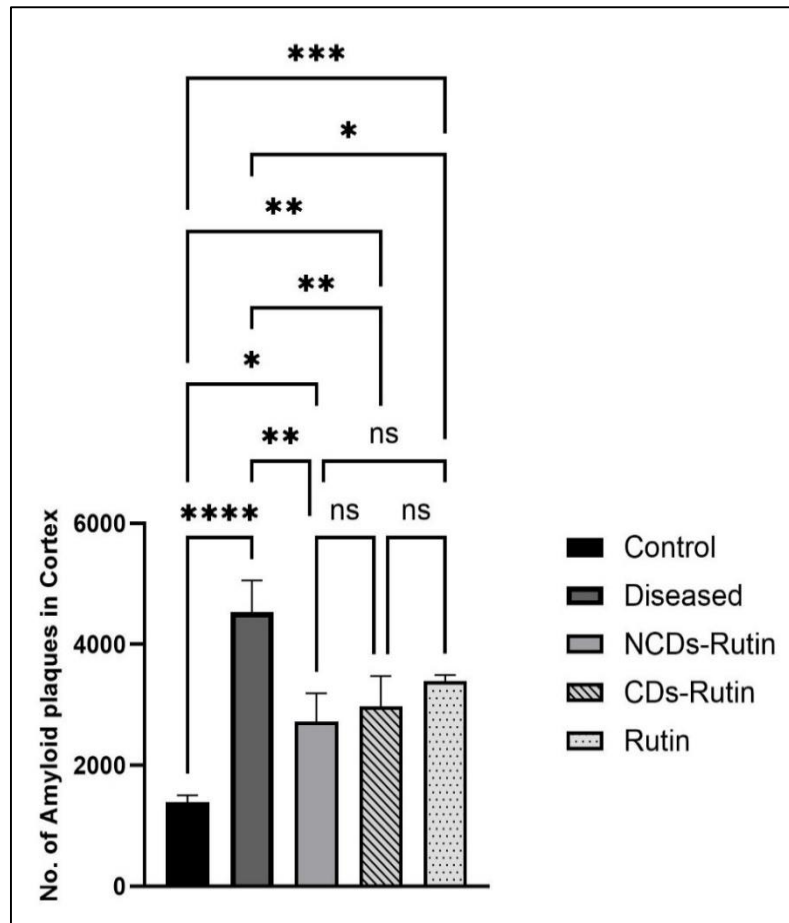
Figure 0.8: Analysis of Amyloid Plaque Accumulation in the Cortex via ThT Staining. The graph compares the number of amyloid plaques in the cortex among five groups. One-way ANOVA, followed by Tukey's multiple comparison test, was used for statistical analysis. Error bars present SEM, 'ns' represent non-significant while *,**, *** and **** represents $p<0.05$, $p<0.01$, $p<0.001$, and $p<0.0001$.

3.3.PCR Results

3.3.1. Gradient PCR Results

To optimize the annealing temperatures for the primers specific to SOD2 and TLR4 genes, gradient PCR was performed using brain tissue samples from rats. The expected amplicon sizes for SOD2 and TLR4 were 113 base pairs and 506 base pairs, respectively. The gradient PCR was conducted over a temperature range of 58°C to 68°C to determine the optimal annealing temperature that minimizes primer-dimer formation and nonspecific binding. The gel electrophoresis results of the gradient PCR are depicted in Figure 18. Distinct bands corresponding to the expected fragment sizes of SOD2 and TLR4 were observed across the temperature gradient. For both SOD2 and TLR4, the most prominent and specific bands without any primer-dimers or nonspecific binding were observed at an annealing temperature of 66°C. At this temperature, the bands for SOD2 were clearly visible at 113 base pairs, while

the bands for TLR4 appeared at 506 base pairs, confirming successful amplification of the target sequences. Temperatures below and above 66°C resulted in either weaker bands or the presence of primer-dimers and nonspecific products, as indicated by additional bands or smearing on the gel. This finding suggests that 66°C is the optimal annealin temperature for the specific amplification of SOD2 and TLR4 without unwanted byproducts.
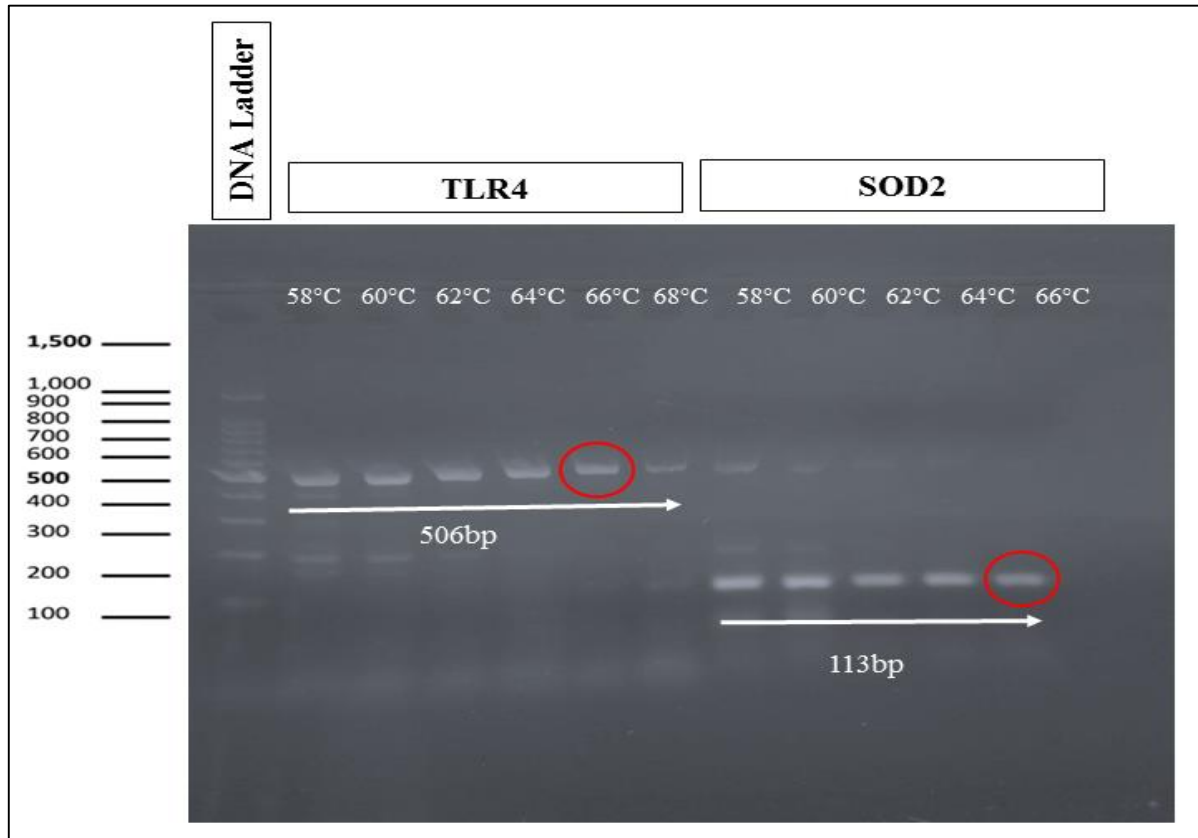
Figure 0.9: Polymerase Chain Reaction (PCR) analysis of rat brain, aimed to evaluate SOD2 and TLR4 gene expression reveals distinct bands on gel electrophoresis corresponding to expected DNA fragment sizes on the temperature range from 58 to 68°C. At an optimized temperature of 66˚C, prominent bands at 113 base pairs indicate successful amplification of SOD2, while bands at 506 base pairs signify successful amplification of TLR4. This demonstrates the effective assessment of gene expression through PCR.

3.3.2. Real-Time PCR Results

3.3.2.1. Relative Expression Level of SOD2

The assessment involved measuring and normalizing the expression of these genes to ß-actin, serving as a housekeeping gene for internal control. The results indicate a distinct modulation in gene expression patterns. The expression of SOD2 was significantly altered among the experimental groups, as illustrated in the figure 19. The disease group, which was induced with AD, showed a notable decrease in SOD2 expression compared to the control group, highlighting the oxidative stress and impaired antioxidant defense mechanisms

associated with Alzheimer's pathology. Conversely, all three treatment groups exhibited a marked increase in SOD2 expression when compared to the disease group. The NCDs-Rutin, CDs-Rutin, and Rutin groups each demonstrated enhanced SOD2 levels, indicating the efficacy of these treatments in upregulating antioxidant defenses and potentially mitigating the oxidative damage associated with AD. Among the treatment groups, the Rutin group exhibited the highest level of SOD2 expression. The NCDs-Rutin group also showed elevated SOD2 expression compared to the control group, though to a lesser extent than the Rutin group. The CDs-Rutin group demonstrated an increase in SOD2 expression compared to the disease group but did not exceed the control group's levels as shown in figure 3.10.
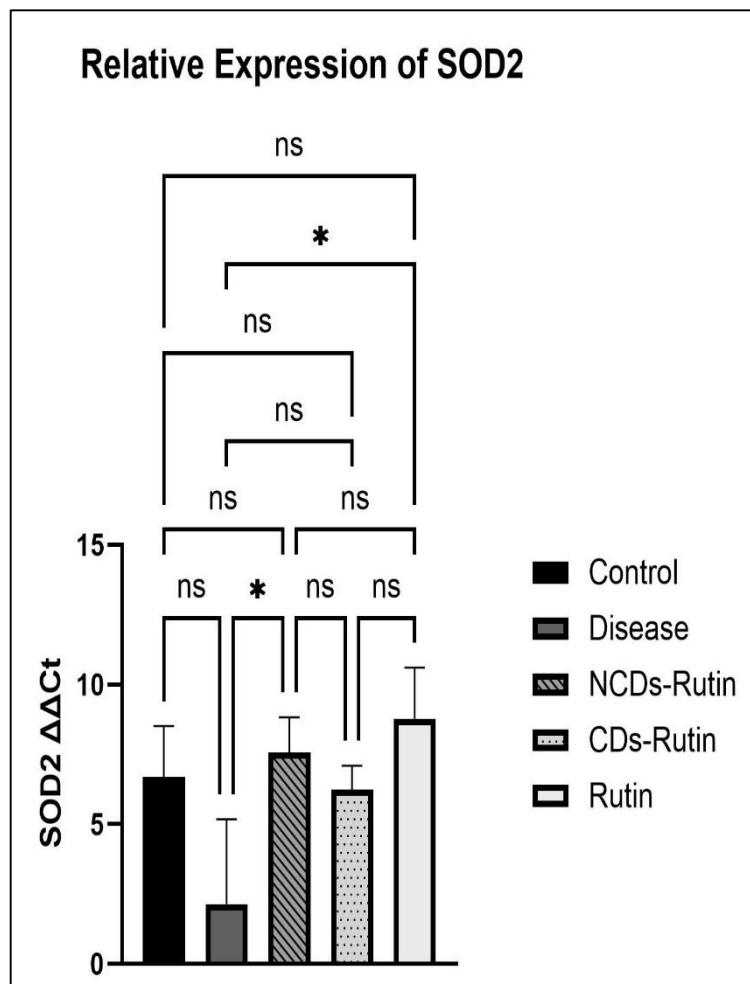
Figure 0.10: Relative expression of SOD2 (Normalization to beta actin). Different experimental groups reveal significant upregulation in antioxidant defense in treatment groups compared to the disease group. Rutin treatment exhibits the highest increase, surpassing control levels, followed by NCDs-Rutin and CDs-Rutin groups. Data are displayed as ±SEM. The non-parametric one-way ANOVA and the Tukey multiple comparison test were used in the statistical analysis. Error bars present SEM, 'ns' represent non-significant while * represents $p<0.05$.

The relative expression of TLR4 was significantly elevated in the disease group compared to the control group ($p < 0.01$). This suggests that AD pathology is associated with an upregulation of TLR4, a pattern recognition receptor involved in innate immunity and inflammation. The treatment groups, which included NCDs-Rutin, CDs-Rutin, and Rutin, exhibited a reduction in TLR4 expression compared to the disease group. However, these reductions were not statistically significant when compared directly to the disease group, indicating that while there was a trend towards normalization, it was not substantial enough to reach significance in this experimental setup. Among the treatment groups, there was no significant difference in TLR4 expression levels. This suggests that all three treatments, NCDs-Rutin, CDs-Rutin, and Rutin, had a similar effect on TLR4 expression, which was not significantly different from each other or the control group.
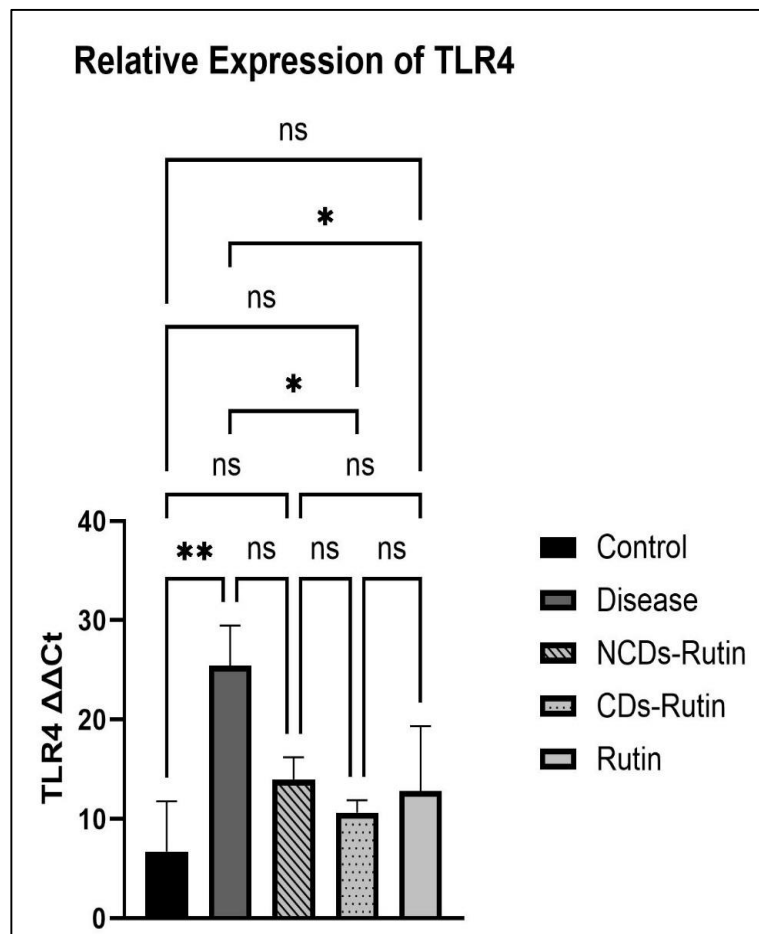
Figure 0.11: Relative expression of TLR4 (Normalization to beta actin). In graph, treatment groups showed significant downregulation compared to disease group. Data are displayed as ±SEM. The non-parametric one-way ANOVA and the Tukey multiple comparison test were used in the statistical analysis. Error bars present SEM, 'ns' represent non-significant while * and ** represents $p<0.05$ and $p<0.01$.

3.4. SDS-PAGE

3.4.1. Coomassie Stained Gel

The gel image presents an SDS-PAGE analysis in which coomassie staining was used to visualize the proteins. The first well was loaded with protein ladder which acts as a reference of molecular weight and the subsequent wells show various experimental groups. Different protein bands are visible on the stained gel, the presence and intensity of these bands vary between groups suggesting differential protein expression. The specific up-regulation and down-regulation in protein targets was determined by using image J software.
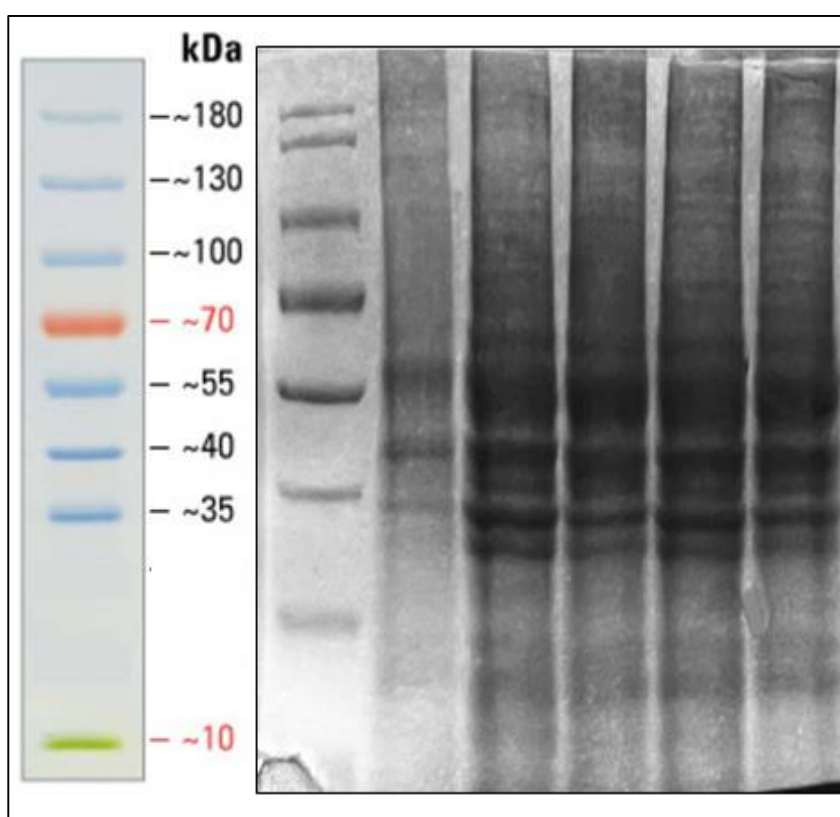
Figure 0.12: Total protein bands on SDS-PAGE stained with coomassie stain. In the first well, protein marker range from 10kDa-180kDa was poured, after that all wells were poured with equal concentration of protein, 20μg/μl. There were five groups, control, diseased, and three treatment groups, NCDs-Rutin, CDs-Rutin and Rutin, each group contains three samples so each well was poured with one sample. After running electrophoresis, gel bands were fixed in a fixative, along with coomassie stain for one hour and destaining for overnight.

3.4.2. Differential Protein Expression in AD

The comparative analysis of protein targets across various molecular weight ranges reveals significant differences between groups. The protein targets were quantified using image

J software, allowing for a detailed comparison of expression level at different molecular weights. The analysis included the measurement of approximate molecular weights of unknown proteins, providing insights into potential roles. This has allowed for the identification of differentially expressed proteins, revealing alterations in protein profiles linked to AD and the outcomes of different treatments were made possible.

The target proteins with molecular weight between 180-130-kDa, 70-55-kDa, 40-35-kDa and at 40-kDa revealed the upregulation in the diseased group compared to control group. Their approximate calculated molecular weights are 140-kDa, 64-kDa, 39-kDa and 40-kDa. Similarly, it was shown that treatment with NCDs-Rutin, CDs-Rutin, and Rutin considerably reduced band intensities in comparison to the disease group. The treatment groups significantly improved, particularly NCDs-Rutin and CDs-Rutin showed better results but there is no significant difference between treatment groups. However, Rutin by itself also significantly reduced the intensity when compared to the disease group, though not as much as treatments with formulations attached to nanoparticles did as shown in figure 3.13A, C, F and G. In contrast, the protein band intensities at 70-kDa, 55-kDa, 10-kDa, between 55-40-kDa and 35-10-kDa was highest in control group and significantly reduced in disease group. Their estimated molecular weights are 70-kDa, 55-kDa, 10-kDa, 47-kDa and 23-kDa. However, the treatment groups improved their level by upregulation. Among the treatment groups, NCDs-Rutin and CDs-Rutin showed better results than Rutin group but there was not significant difference between all treatment groups, figure 3.13 B, D, E, H and I.
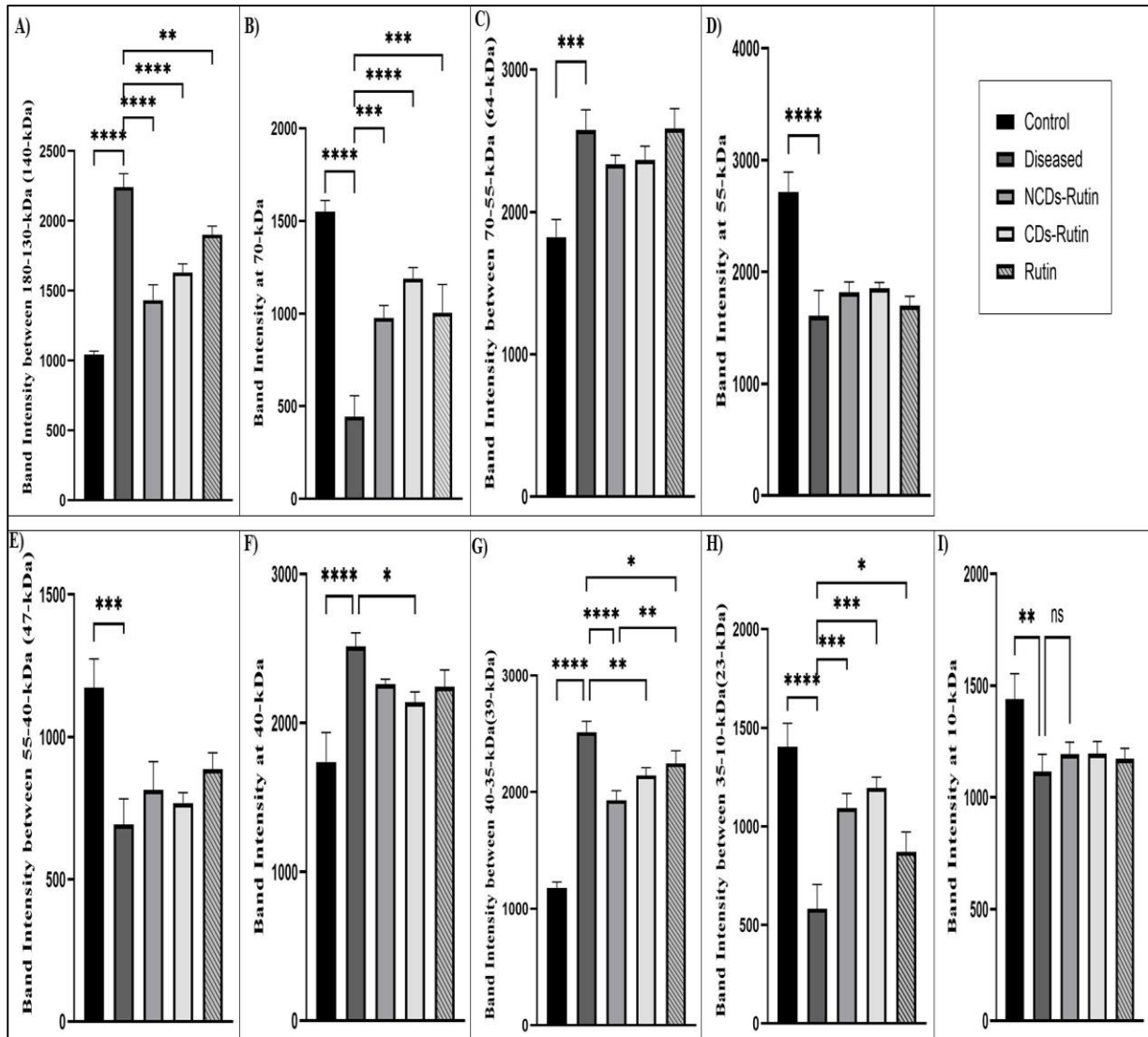
Figure 0.13: Differentially regulated protein bands of control, diseased and treatment group were measured. (A) Protein targets were measured against molecular weight between 180-130kDa where NCDs-Rutin treatment group is showing significant results than other two treatment groups, also it is significant than disease group, (B) at 70kDa, NCDs-Rutin and Rutin group is significantly increased compared to disease group, (C) between 70-55kDa, in which NCDs-Rutin and CDs-Rutin is giving better result than Rutin group and also reduced level from diseased group, (D) at 55kDa, treatment is showing better results than diseased but not signicantly improved, (E) between 55-40kDa, treatment groups are giving comparatively better results than diseased group, while Rutin is showing significant result among treatment groups, (F) at 40kDa, here CDs-Rutin is showing improvement compared to other treatment groups, while in comparison to disease group, all treatment groups is showing reduced level but not as significant, (G) protein intensity between 40-35kDa, treatment groups are significantly showing better results than diseased group, NCDs-Rutin has improved its level than other treatment groups, (H) between 35-10kDa, treatment groups are significantly increased compared to disease group, while CDs-Rutin treatment group is showing significant results among treatment groups, (I) protein level at 10-kDa where disease group reduced it level than control, treatment groups showed least improvement and it was not significant compared to diseased group. Data are displayed as ±SEM. The non-parametric one-way ANOVA and the Tukey multiple comparison test were used in the statistical analysis. Error bars present SEM, *, **, *** and **** represents p<0.05, p<0.01, p<0.001, and p<0.0001.

CHAPTER 4: DISCUSSION

Significant attempts have been used in studying the pathogenesis of AD for last decades, and amyloid hypothesis is currently holding by most of the laboratories and clinics around the globe. Some of them involves drugs designed to increase Aβ catabolism or decrease its synthesis: reported to decrease Aβ in animal models or in patients with AD, but did not yield favourable results on clinical outcomes of the disease. However, failure does not mean the stop of clinical trial or thinking the Aβ hypothesis is wrong. In the present study we have explained the effectiveness of Rutin, a small molecular which could significantly improve the learning and memory deficit in rats and thus it is a potential therapeutic drug for treatment of AD(Selkoe & Hardy, 2016). Besides, to compare the efficacy of Rutin the sample Rutin-bound nanoparticles, NCDs and CDs were also synthesized and studied. Rutin whereby it acts as phenolic anti-oxidant, has several pharmacological effects under several pathological conditions.

The compounds of Rutin show many pharmacological actions such as anti-oxidant, anti-inflammatory, and neuroprotective. Due to these properties, Rutin may be considered as a potential drug for AD treatment, as oxidative stress and inflammation played crucial role in the development of AD. Research has shown that Rutin on one hand plays the role of a free radical scavenger and on the other hand, it stimulates the function of the endogenous antioxidant enzymes. Also, it has been indicated that Rutin downregulates the production of pro-inflammatory cytokines and decreases microglial and astrocytic activation. According to a study it was found that the beneficial effects of Rutin on Aβ, oxidative stress, and neuroinflammation lead to the improvement of spatial memory in AD mice (Xu et al., 2014).

Rutin modulates antioxidant enzymes such as, SOD, catalase, and glutathione peroxidase and therefore exhibits the efficacy to cope up the oxidative stress. It is an antioxidant that mops up free radicals such as reactive oxygen species (ROS) and reactive nitrogen species which are increased in AD and which cause harm to neurons. It also helps to suppress inflammation through down regulation of nuclear factor-kappa B (NF-κB) which is a well-known mediator of inflammation. Through the inhibition of NF-κB, Rutin decreases the production of pro-inflammatory cytokines, viz, TNF-α, IL-1β as well as interleukin-6 (IL-6). It also assists in modulating the inflammatory response that may harm neurons thus playing a major role in reducing inflammation to the neurons (Ganeshpurkar & Saluja, 2017). However, it has a low bioavailability and cannot readily cross blood-brain barrier (BBB) which becomes

a problem in certain clinical cases. The BBB is a very tight barrier involved in defending the brain against toxic substances while controlling the movement of the molecules into and out of the brain. But this protective function complicates the delivery of many therapeutic agents to the CNS. Since Rutin appears to be highly hydrophilic and possesses a large molecular mass, it encounters notable barriers in its ability to cross into the BBB and deliver the needed concentrations necessary for exerting the medicine's therapeutic impact (Xu et al., 2014),

Due to this limitation, further studies have been conducted using nanoparticle-based drug delivery system in order to promote the delivery of Rutin to the brain. Nanoparticles are very small particles which can be synthesized to encapsulate therapeutic materials and help them to cross barriers such as the BBB. Several classes of nanoparticles, for example liposomal, polymeric and solid lipid nanoparticles have been contemplated for their exhibition in encapsulating Rutin and enhancing the pharmacokinetic behaviour of the material (Hersh et al., 2022). In the present investigation, Rutin-conjugated nanoparticles were used to investigate and compare the extent of delivery of Rutin in an Alzheimer's model of rat. The use of nanoparticles offers several advantages: They can help to preserve Rutin and prevent its decline, increase its solubility and maintain its gradual supply in the organism. Besides, the used nanoparticles can be surface modified with targeting ligands that help the nanoparticles to be taken up by the Brain endothelial cells and transported across the BBB through receptor mediated transcytosis (Song et al., 2023).

Behavioral testing was conducted to evaluate the cognitive and memory functions in the rat models of AD using four different tests: Such test includes the MWM, Y-Maze, Open Field, and NOR. The MWM test is an effective and common employed behavioral test for staging spatial learning and memory in rodents. The MWM test in the present study is the process of training the rats to find the submerged platform in a tank filled with water for days. The current findings showed that escape latency and the distance traveled by rats of the AD group were significantly higher compared to the control group; therefore, it can be deduced that AD interfered with the cognitive function of the disease model rats. Nevertheless, rats which received Rutin significantly decreased the escape latency and path length proving the enhancement of the spatial learning and memory abilities. Particularly, the escape latency of the rats subjected to Rutin was reduce from about 70s before training to about 40s by the end of training. In another study Rutin enhanced cognitive and mnemonic processes in different animal models of neurodegeneration during this test (Sun et al., 2021).

NCDs-Rutin further ameliorated the rats' condition, the escape latencies being reduced to 35 ± 1.52 seconds thereby confirming the better efficacy of Rutin when administered through NCDs. This is supported by other works showing that drug delivery formed from nanoparticles offered better delivery and effectiveness. It is important to special underline the rats treated with CDs-Rutin by which the average escape latency has been improved to be close to the control group's level 30 seconds together with good path length. This implies that CDs contribute a lot to the bioavailability and performance of Rutin in combating cognitive impairment in AD.

The Y Maze test measures the working memory and the cognitive flexibility in the rodents. Hence, in this study, AD induced rats performed much worse than the control rats in terms of the working memory since they displayed a significantly low number of L1 group spontaneous alternation behavior. More specifically, AD-induced rats got about 40 percent of the points that concern the spontaneous alternation percentage, while the control rats got 70 percent of such a type of points. After the treatment with Rutin the rats demonstrated the increase in the level of the spontaneous alternation behavior up to the 60%. These outcomes correspond with earlier investigations where it was discovered that Rutin enhanced effectiveness in the Y Maze test, which is in models of cognitive deficits (Sun et al., 2021). The rats in the NCDs-Rutin group exhibited a heightened reaction with a slight increase of the behavioral test for spontaneous alternation to about 65%. This implies that the Rutin neuroprotection by NCDs is improved. The greatest enhancement was noticed in groups receiving CDs-Rutin, the spontaneous alternation activity was 72.8 percent. This shows that besides the effect of CDs-Rutin in replenishing the working memory, its impact is more superior than that of Rutin alone on the working memory performance of the participants. This is in concord with literature supporting the notion that nanoparticle aid in the enhancement of drug efficiency and their delivery to the brain sites.

Open field test is commonly applied in the evaluation of ambulatory activity and also has a role in measuring of anxiety levels in rodents. Our investigation showed that for AD-induced rats, the time spent on the central area of the open field was significantly decreased suggesting the increased anxiety-like behavior and the reduced exploration that is in concordance with the previous studies that implicated Alzheimer's pathology with increased anxiety and locomotor dysfunction (Sun et al., 2021). On the time spent in the central area, there was an indication that the treatment groups that included Rutin and NCDs-Rutin had a

significant improvement based on the disease group. This change indicates a decrease in anxiolytic activity and an increase in activity exploration. Consequently, in another research, where flavonoid therapeutic where the effects of Rutin was beneficial in models of neurodegenerative diseases included reduced anxiety and increased locomotor activity. These findings are supported by our results and suggest that Rutin as well as formulations containing Rutin nanoparticles may be effective in reducing anxiety and increasing the exploratory activity in the models of AD (Horka et al., 2024).

NOR test represents a measure of recognition memory, which is based on the Hippocampus and, more specifically, hippocampal dependent memory working; this is severely affected in AD. Thus, our findings where AD induced rats took lesser time exploring the novel object compared with control rats are consistent with the literature databases and confirm the effect of AD on recognition memory. The treated rats using the Rutin, NCDs-Rutin, and CDs-Rutin showed significant improvement in the recognition memory as compared to the disease group, the rats spent more time exploring the novel object than the disease group. Thus, CDs-Rutin exhibited the maximum improvement among the treatment groups and rose even higher than the other treatment groups and was almost on par with control. This means that by formulating CDs, the bioavailability and efficiency of Rutin for the treatment of cognitive impairment maybe boosted (Guo et al., 2022).

Morphological analysis is incredibly valuable as it includes information on structural shifts and the signs of pathological processes in AD. Several changes in the tissue characteristics occur in these cases, including; H&E staining and ThT staining are some of the most common techniques used in evaluating such changes. AD models in cultures generally show some sizable changes in the histopathological features using H&E staining which includes; decrease in the number of neurons, increase in cells and nucleus, and vacuolated neuron. These changes are consistent with the protracted neuropathological processes in which AD is constituted (Zerrouki et al., 2021). In the diseased group, the cerebral atrophy was pronounced while for the respective groups treated with, especially the NCDs-Rutin treatment; significant enhancement was observed. Based on these findings, NCDs-Rutin group had denser neuronal elements and less cell lesion, suggestive of neuroprotection against NCDs. These results corroborate other studies that propose that flavonoids therapies, especially those related to nanoparticle, can improve neuronal viability and decrease the pathophysiological hallmarks of AD.

ThT staining has high specificity for amyloid plaques which is one of the hall marks of AD. It did depict that the diseased set of the patients had a higher density of amyloid plaques and the groups that received treatment were found to have a lesser deposition of these plaques. According to the treatments done in this study, it was evident that NCDs-Rutin has the most pronounced effect in reducing the formation of amyloid plaques compared to CDs-Rutin and Rutin. hese findings are in line with other published works that indicated that Rutin and its nanoparticle formulations may be useful in combating amyloid load. This achieved clearance of amyloid plaques can be associated with antioxidant and anti-inflammatory effect of Rutin and also due to optimization of the delivery and bioavailability by using the nanoparticles conjugation (Sun et al., 2021).

After the histological assessment, a molecular assessment of gene expression of SOD2 and TLR4 was done since these both are inflammatory markers related to oxidative stress in AD. In the mitochondria superoxide anions are neutralized by SOD-2. There have been 16 AD mouse models having low SOD-2 which results in early cognitive decline and elevated brain Aβ. Quantitative changes of an antioxidant enzyme SOD 2 in an AD model were the measure of oxidative stress across the experimental groups. As for the SOD2, the result showed that expression in the disease group was significantly lower than that in the control group, which illustrated the fact that the antioxidant defense deteriorated in AD based on the previous study that pointed out increased oxidative stress and mitochondrial dysfunction in AD. Reduced quantities of SOD2 in the disease group were critical due to the oxidative damage seen in the neurodegenerative diseases and supported oxidative stress as a factor in AD (Wiener et al., 2007).

The treatment groups receiving Rutin, NCDs-Rutin, and CDs-Rutin demonstrated significant upregulation of SOD2 expression compared to the disease group. Among them, Rutin-treated group possessed the highest expression of SOD2 which is still higher than that of the control. This huge up regulation suggests there was a good anti oxidative response this could be due to free radical scavenging of Rutin or the effects of Rutin on antioxidant enzymes. The level of SOD2 was also up-regulated in the NCDs-Rutin group, which was higher than the control, but lower than the Rutin group; This demonstrates that the nano-carrier formulation of Rutin increases its bioavailability and effectiveness. CDs-Rutin treatment significantly upregulated SOD2 expression to $135 \pm 3.87\%$ of the Con group, which was less effective than Rutin and NCDs-Rutin, but better than the disease group. Overall, the current studies imply

that Rutin as well as its nanocarriers could help in fortifying the antioxidant capacity and combating oxidative stress in AD. Concerning these findings, it can be concluded that the observed neuroprotective effects of Rutin in the present study are mainly due to its antioxidant activities. Literatures have also revealed that flavonoids such as Rutin modulate the endogenous antioxidant enzyme which helps to protect the neurons from oxidative stress and hence increase the neuronal survivability in the AD models. The increased efficiency that is usually associated with Rutin particles can therefore be explained by better dispersion and superior stability that allows for increased effect. In essence, therefore, our results support the existing literature and give hope for the therapeutic effectiveness of Rutin especially the nano-formulated to mitigate oxidative stress in AD.

Comparing the data on TLR4 levels in different experimental groups can be useful for understanding the inflammatory changes in the context of AD and possible treatments. Indeed, in our study the disease group has higher levels of TLR4 than the control group, consistent with previous studies that associate increased TLR4 signaling to neuroinflammation in AD. TLR4 as an essential part of the immune sensing participates in signaling in response to PAMPs and DAMPs. This was evidenced by the high expression level of TLR4 in the disease group as compared to the control group, implying that neuroinflammation is more pronounced in patients with the disease as expected in AD. The treatment groups that received NCDs-Rutin, CDs-Rutin, and Rutin all exhibited a tendency in the change of TLR4 expression, but not a significant difference when compared to the disease group. This is an important indication of possible anti-inflammatory effects of these treatments. Being a well-established flavonoid, Rutin is scientifically characterized as having anti-inflammatory and antioxidant activities, all of which could explain the observed TLR4 modulatory effect of the compound. Specifically, the NCDs and CDs conjugated with Rutin contain nanoparticles that make Rutin better in delivery and therapeutical effect (Wu et al., 2022).

In molecular weight range of 180-130 kDa, significant differences in the expression of the protein were observed between the control, diseased, and treatment groups. The band intensity of the diseased group was significantly higher ($p < 0.01$) than that of the control group, indicating upregulation of protein in Alzheimer's disease. This range contain proteins like tau or APP that are linked to neurodegeneration. Protein levels in the NCDs-Rutin treated group were significantly lower ($p < 0.05$), and the difference was statistically significant when compared to the control level. Rutin as well as CDs-Rutin reduced protein expression (p <

0.05). AD affects the production of numerous proteins, including those that may have functions in cellular maintenance or signaling like tubulin or other structural proteins, which are down-regulated (Cyske et al., 2023). The control group showed a larger intensity at 70 kDa than the diseased group ($p < 0.0001$). The significant decline was observed in the disease group highlights the pathologically detrimental consequences of Alzheimer's on the human brain's proteome. When cells that are otherwise slowed by the disease are treated with NCDs-Rutin, the proteome protein abundance in this molecular weight class increases to nearly normal levels ($p < 0.01$), suggesting that this formulation may aid in the recovery of some normal functions. Similar to NCDs-Rutin, CDs-Rutin showed less reduction but still highly significant change in protein levels when compared to control levels, $p < 0.01$ (Nguyen et al., 2024).

The diseased group's protein level was considerably greater in the 70–55 kDa range than the control group's ($p < 0.001$), which may point to an increase in the production of proteins linked to neuroinflammatory or stress response. These molecular weight ranges may have connections to proteins, such as heat shock proteins (HSPs), or immune response components, which are often linked to Alzheimer's disease (Selkoe, 2004). Similarly, administering NCDs-Rutin significantly decreased band intensity to the closest baseline status ($p < 0.0001$), suggesting that the drug could counteract the disease's influence on protein levels. Rutin and CDs-Rutin similarly reduced protein expression ($p < 0.05$), however the effect was not as significant as it was with NCDs-Rutin. Protein expression is highest in the control group at 55 kDa, with a mean density of roughly 3000. In contrast to the control group, the diseased group exhibits significantly lower levels of protein expression together with higher band intensities ($p < 0.0001$). When comparing the effects of CDs-Rutin and NCDs-Rutin, a considerable restoration in protein expression is detected; nevertheless, the alterations that are found are not statistically significant when compared to the diseased group ($p > 0.05$). There is also a seeming similarity with Rutin alone, since there was no difference in the protein intensity levels between the parts treated with Rutin alone and the sections with bound Rutin nanoparticles (Schaffar et al., 2004).

The control group has the highest intensity values (mean intensity of around 1000 units) in the molecular weight range of 55-40-kDa. In contrast, the diseased group exhibits a significant drop in protein expression in this molecular weight range ($p < 0.001$). When compared to the diseased group, the current treatment with NCDs-Rutin and CDs-Rutin slightly increases protein intensity, but the difference is not statistically significant ($p > 0.05$).

Comparing the Rutin treatment group to the diseased group and the nanoparticle-bound therapies reveals no difference in the intensity level, but it does demonstrate an increase similar to the findings on the increase in intensity of disease pathogenicity. When compared to the control group, the diseased group at 40 kDa molecular weight displayed an enhanced band density (****$p<0.0001$), which may indicate that proteins are up-regulated at this molecular weight in the Alzheimer's disease (AD) model. The tau protein and APP fragments are the proteins that are observed to be moved within the 40 kDa range in the majority of AD cases. The band intensities of the NCDs-Rutin and CDs-Rutin groups were relatively modest, and they were lower than those of the sick group, while there was no discernible difference. Earlier, controlled alterations were noted in the group receiving Rutin, where there appeared to be a partial reversal of typical protein concentrations (Walsh & Selkoe, 2004).

CHAPTER 5: SUMMARY OF RESEARCH WORK

AD is a neurological disorder that worsens with time and impairs cognitive abilities generally as well as memory and spatial awareness. The development of Aß plaques and neurofibrillary tangles in the brain, which result in neuronal drop off and brain shrinkage, is the cause of this kind of dementia. Over the past ten years, the use of nanoparticles has increased, providing a means of improving therapeutic targeting and efficacy in the treatment of neurodegenerative diseases. In an AD rat model, the objective of this work is to assess the level of neuroprotection induced by the bioactive flavonoid Rutin and its nano-vehicles. Rutin is widely known for its neuroprotective qualities, anti-inflammatory characteristics, and antioxidant activity. However, significant issues with its low solubility and bioavailability make it difficult to get enough dosages of the medication to the target organ, the brain, which hinders its clinical application. This work aimed to use CDs and NCDs as Rutin carriers in an effort to overcome these difficulties.

The male Wistar Han rats used as the experimental model for this experiment. Using D-galactose and $AlCl_3$ as interventions, an AD model was created. For a specific period of time, the prescribed treatment plans were followed, and a series of behavioral tests was administered to evaluate cognitive function, spatial learning and memory, motor activity, anxiety-like and exploratory behavior, and recognition memory. Moreover, PCR analysis using the SOD2 and TLR4 primers was performed to examine the molecular basis of these behavioral improvements. At 66°C, when these primers were developed, no primer dimer formation or sequences other than target sequences occurred. Additionally, histological staining such as H&E was used to examine overall tissue morphology and ThT was used to examine the development of amyloid plaques. H&E staining of the AD-induced rats' hippocampal and cortical structural disarray and loss of neurons were both validated. However, Rutin and its nanoparticle formulations helped to partially offset these histopathological alterations, and the CDs-Rutin group showed the highest level of protection. Therefore, ThT staining supported the reduction in amyloid plaque observed in the Rutin and its nanoparticle-treated groups, indicating that these treatments may be able to avert the consequences of AD. These findings lead the research team to assume that Rutin, particularly bounded with nanoparticles, may be developed into a treatment for AD.

CHAPTER 6: CONCLUSION AND FUTUTRE RECOMMENDATIONS

AD is still considered one of the most significant issues in the study of neurodegenerative illnesses because of its intricate etiology, which involves amyloid-beta plaques, neurofibrillary tangles, and numerous neuronal deaths. In light of this, the current study's specific goal was to use an animal model of AD to examine the preventive effects of Rutin and its nano-carrier systems, which include CDs and NCDs. This study provides evidence that these treatments may be able to mitigate cognitive function deficits and lessen the neuropathological changes associated with AD. Numerous research has focused on Rutin because of its neuroprotective, anti-inflammatory, and antioxidant properties. However, problems with low solubility and thus low bioavailability limit its clinical applicability. Because Rutin's solubility, stability, and ability to pass the blood-brain barrier can all be greatly enhanced by nanoparticles, the challenges associated with Rutin use have also stimulated the idea of employing them as delivery systems. This viewpoint presents a possible innovation for augmenting the therapeutic effects that Rutin is intended to have in the management of AD.

Behavioral tests revealed that the significantly low cognitive functions had been spared, and all therapy groups showed improvement as compared to the AD-induced group. The fact that the CDs-Rutin group saw the greatest increase, however, suggests that CDs play a significant role in enhancing Rutin's bioavailability and effectiveness. The molecular details for the specific and non-specific binding, as well as the associated molecular pathologies, were shown by PCR studies for SOD2 and TLR4. Thioflavin T (ThT) staining and histological inspection, which also showed that neuronal loss and amyloid plaque formation were significantly lower in the tested groups, supported this.

The potential usefulness of nanoparticles in the treatment of AD is demonstrated by the ability of CDs-Rutin nanoparticle formulations to boost drug efficacy. These formulations have the potential to be useful therapeutic agents since they improve cognitive function and reduce neuropathological changes. Consequently, it can be said that CDs-Rutin performed better than the other formulations, opening the door to further research and development of this compound as a prospective remedy.

Based on the findings of this study, several directions, nonetheless, might need further investigation in order to support the theory of the effectiveness of Rutin in treating AD and the efficacy of its nanoparticle forms. Initially, thorough analyses of the molecular mechanisms

underlying the protective benefits of the aforementioned treatments are required, utilizing particular markers. It will be feasible to create more targeted and potent treatment plans and optimize the dosing regimens for Rutin and its nanoparticles if the precise mechanisms by which they function are clarified. Moreover, longitudinal studies must be carried out to assess the durability of identified favorable trends and potential negative consequences. Long-term rodent administration of these therapies in these animal models will provide crucial information on their effectiveness and toxicity for the planning of potential clinical trials.

Additionally, more research ought to be done on the potential for larger-scale nanoparticle manufacturing and replication. To make it function clinically, it is crucial to adhere to the exact quality and performance of the created nanoparticles. Thus, thorough investigations into different types of nanoparticles and their suitability for Rutin delivery could contribute to increasing the potential applications of this drug. Expanding the scope to include additional neurodegenerative disease models, however, would facilitate a more thorough comprehension of the broader applicability of these curative methods. Therefore, the generality and stability of the effects stated above will be revealed by additional comparative studies using animal models with varying degrees of AD pathology and different kinds of nanoparticulate Rutin. The final and most important milestone is the switch from *in vitro*/*in silico* to *in vivo*. The development and implementation of clinical trials will necessitate interdisciplinary collaboration to validate the application of these medicines in humans. Nevertheless, a number of steps will need to be taken in order to attempt translating these findings into the clinic, such as establishing the kind of endpoints to be evaluated, patients to be targeted, and regulatory criteria.

REFERENCES

A. Armstrong, R. (2019). Risk factors for Alzheimer's disease. *Folia Neuropathologica*, *57*(2), 87–105. https://doi.org/10.5114/fn.2019.85929

Agrahari, V. (2017). The exciting potential of nanotherapy in brain-tumor targeted drug delivery approaches. *Neural Regeneration Research*, *12*(2), 197.

Alonso, A. D., Li, B., Grundke-Iqbal, I., & Iqbal, K. (2008). Mechanism of Tau-Induced Neurodegeneration in Alzheimer Disease and Related Tauopathies. *Current Alzheimer Research*, *5*(4), 375–384. https://doi.org/10.2174/156720508785132307

Apostolova, L. G. (2016). Alzheimer Disease: *CONTINUUM: Lifelong Learning in Neurology*, *22*(2, Dementia), 419–434. https://doi.org/10.1212/CON.0000000000000307

Ballard, C., Gauthier, S., Corbett, A., Brayne, C., Aarsland, D., & Jones, E. (2011). Alzheimer's disease. *The Lancet*, *377*(9770), 1019–1031. https://doi.org/10.1016/S0140-6736(10)61349-9

Bromley-Brits, K., Deng, Y., & Song, W. (2011). Morris Water Maze Test for Learning and Memory Deficits in Alzheimer's Disease Model Mice. *Journal of Visualized Experiments*, *53*, 2920. https://doi.org/10.3791/2920

Brookmeyer, R., Johnson, E., Ziegler-Graham, K., & Arrighi, H. M. (2007). Forecasting the global burden of Alzheimer's disease. *Alzheimer's & Dementia*, *3*(3), 186–191.

Budzynska, B., Faggio, C., Kruk-Slomka, M., Samec, D., Nabavi, S. F., Sureda, A., Devi, K. P., & Nabavi, S. M. (2019). Rutin as Neuroprotective Agent: From Bench to Bedside. *Current Medicinal Chemistry*, *26*(27), 5152–5164. https://doi.org/10.2174/0929867324666171003114154

Chen, G., Xu, T., Yan, Y., Zhou, Y., Jiang, Y., Melcher, K., & Xu, H. E. (2017). Amyloid beta: Structure, biology and structure-based therapeutic development. *Acta Pharmacologica Sinica*, *38*(9), 1205–1235. https://doi.org/10.1038/aps.2017.28

Cipriani, G., Dolciotti, C., Picchi, L., & Bonuccelli, U. (2011). Alzheimer and his disease: A brief history. *Neurological Sciences*, *32*(2), 275–279. https://doi.org/10.1007/s10072-010-0454-7

Colin, J., Thomas, M. H., Gregory-Pauron, L., Pinçon, A., Lanhers, M.-C., Corbier, C., Claudepierre, T., Yen, F. T., Oster, T., & Malaplate-Armand, C. (2017). Maintenance of membrane organization in the aging mouse brain as the determining factor for preventing receptor dysfunction and for improving response to anti-Alzheimer treatments. *Neurobiology of Aging*, *54*, 84–93.

Corrada, M. M., Brookmeyer, R., Berlau, D., Paganini-Hill, A., & Kawas, C. H. (2008). Prevalence of dementia after age 90: Results from The 90+ Study. *Neurology*, *71*(5), 337–343. https://doi.org/10.1212/01.wnl.0000310773.65918.cd

Cras, P., Kawai, M., Lowery, D., Gonzalez-DeWhitt, P., Greenberg, B., & Perry, G. (1991). Senile plaque neurites in Alzheimer disease accumulate amyloid precursor protein. *Proceedings of the National Academy of Sciences*, *88*(17), 7552–7556. https://doi.org/10.1073/pnas.88.17.7552

Cristea, I. M., Gaskell, S. J., & Whetton, A. D. (2004). Proteomics techniques and their application to hematology. *Blood*, *103*(10), 3624–3634. https://doi.org/10.1182/blood-2003-09-3295

Cummings, J., Ritter, A., & Zhong, K. (2018). Clinical trials for disease-modifying therapies in Alzheimer's disease: A primer, lessons learned, and a blueprint for the future. *Journal of Alzheimer's Disease*, *64*(s1), S3–S22.

Cyske, Z., Gaffke, L., Pierzynowska, K., & Węgrzyn, G. (2023). Tubulin Cytoskeleton in Neurodegenerative Diseases–not Only Primary Tubulinopathies. *Cellular and Molecular Neurobiology*, *43*(5), 1867–1884. https://doi.org/10.1007/s10571-022-01304-6

De-Paula, V. J., Radanovic, M., Diniz, B. S., & Forlenza, O. V. (2012). Alzheimer's Disease. In J. R. Harris (Ed.), *Protein Aggregation and Fibrillogenesis in Cerebral and Systemic Amyloid Disease* (Vol. 65, pp. 329–352). Springer Netherlands. https://doi.org/10.1007/978-94-007-5416-4_14

Dubois, B., Hampel, H., Feldman, H. H., Scheltens, P., Aisen, P., Andrieu, S., Bakardjian, H., Benali, H., Bertram, L., Blennow, K., Broich, K., Cavedo, E., Crutch, S., Dartigues, J., Duyckaerts, C., Epelbaum, S., Frisoni, G. B., Gauthier, S., Genthon, R., … Proceedings of the Meeting of the International Working Group (IWG) and the American Alzheimer's Association on "The Preclinical State of AD"; July 23, 2015; Washington DC, USA.

(2016). Preclinical Alzheimer's disease: Definition, natural history, and diagnostic criteria. *Alzheimer's & Dementia*, *12*(3), 292–323. https://doi.org/10.1016/j.jalz.2016.02.002

Ferri, C. P., Prince, M., Brayne, C., Brodaty, H., Fratiglioni, L., Ganguli, M., Hall, K., Hasegawa, K., Hendrie, H., & Huang, Y. (2005). Global prevalence of dementia: A Delphi consensus study. *The Lancet*, *366*(9503), 2112–2117.

Fonseca-Santos, B., Gremião, M. P. D., & Chorilli, M. (2015). Nanotechnology-based drug delivery systems for the treatment of Alzheimer's disease. *International Journal of Nanomedicine*, 4981–5003.

Ganeshpurkar, A., & Saluja, A. K. (2017). The Pharmacological Potential of Rutin. *Saudi Pharmaceutical Journal*, *25*(2), 149–164. https://doi.org/10.1016/j.jsps.2016.04.025

Goedert, M., & Spillantini, M. G. (2006). A century of Alzheimer's disease. *Science*, *314*(5800), 777–781.

Guo, F., Li, Q., Zhang, X., Liu, Y., Jiang, J., Cheng, S., Yu, S., Zhang, X., Liu, F., Li, Y., Rose, G., & Zhang, H. (2022). Applications of Carbon Dots for the Treatment of Alzheimer's Disease. *International Journal of Nanomedicine*, *Volume 17*, 6621–6638. https://doi.org/10.2147/IJN.S388030

H. Ferreira-Vieira, T., M. Guimaraes, I., R. Silva, F., & M. Ribeiro, F. (2016). Alzheimer's disease: Targeting the Cholinergic System. *Current Neuropharmacology*, *14*(1), 101–115. https://doi.org/10.2174/1570159X13666150716165726

Habtemariam, S. (2016). Rutin as a natural therapy for Alzheimer's disease: Insights into its mechanisms of action. *Current Medicinal Chemistry*, *23*(9), 860–873.

Hampel, H., Mesulam, M.-M., Cuello, A. C., Farlow, M. R., Giacobini, E., Grossberg, G. T., Khachaturian, A. S., Vergallo, A., Cavedo, E., Snyder, P. J., & Khachaturian, Z. S. (2018). The cholinergic system in the pathophysiology and treatment of Alzheimer's disease. *Brain*, *141*(7), 1917–1933. https://doi.org/10.1093/brain/awy132

Hanasaki, Y., Ogawa, S., & Fukui, S. (1994). The correlation between active oxygens scavenging and antioxidative effects of flavonoids. *Free Radical Biology and Medicine*, *16*(6), 845–850.

Henstridge, C. M., Pickett, E., & Spires-Jones, T. L. (2016). Synaptic pathology: A shared mechanism in neurological disease. *Ageing Research Reviews*, *28*, 72–84. https://doi.org/10.1016/j.arr.2016.04.005

Hersh, A. M., Alomari, S., & Tyler, B. M. (2022). Crossing the Blood-Brain Barrier: Advances in Nanoparticle Technology for Drug Delivery in Neuro-Oncology. *International Journal of Molecular Sciences*, *23*(8), 4153. https://doi.org/10.3390/ijms23084153

Holman, J. D., Dasari, S., & Tabb, D. L. (2013). Informatics of Protein and Posttranslational Modification Detection via Shotgun Proteomics. In M. Zhou & T. Veenstra (Eds.), *Proteomics for Biomarker Discovery* (Vol. 1002, pp. 167–179). Humana Press. https://doi.org/10.1007/978-1-62703-360-2_14

Horka, P., Langova, V., Hubeny, J., Vales, K., Chrtkova, I., & Horacek, J. (2024). Open field test for the assessment of anxiety-like behavior in Gnathonemus petersii fish. *Frontiers in Behavioral Neuroscience*, *17*, 1280608. https://doi.org/10.3389/fnbeh.2023.1280608

Hrnkova, M., Zilka, N., Minichova, Z., Koson, P., & Novak, M. (2007). Neurodegeneration caused by expression of human truncated tau leads to progressive neurobehavioural impairment in transgenic rats. *Brain Research*, *1130*, 206–213. https://doi.org/10.1016/j.brainres.2006.10.085

Jain, M., Dhariwal, R., Patil, N., Ojha, S., Tendulkar, R., Tendulkar, M., Dhanda, P. S., Yadav, A., & Kaushik, P. (2023). Unveiling the Molecular Footprint: Proteome-Based Biomarkers for Alzheimer's Disease. *Proteomes*, *11*(4), 33. https://doi.org/10.3390/proteomes11040033

Javed, H., Khan, M. M., Ahmad, A., Vaibhav, K., Ahmad, M. E., Khan, A., Ashafaq, M., Islam, F., Siddiqui, M. S., & Safhi, M. M. (2012). Rutin prevents cognitive impairments by ameliorating oxidative stress and neuroinflammation in rat model of sporadic dementia of Alzheimer type. *Neuroscience*, *210*, 340–352.

Kametani, F., & Hasegawa, M. (2018). Reconsideration of Amyloid Hypothesis and Tau Hypothesis in Alzheimer's Disease. *Frontiers in Neuroscience*, *12*, 25. https://doi.org/10.3389/fnins.2018.00025

Kitamura, Y., Usami, R., Ichihara, S., Kida, H., Satoh, M., Tomimoto, H., Murata, M., & Oikawa, S. (2017). Plasma protein profiling for potential biomarkers in the early diagnosis of Alzheimer's disease. *Neurological Research*, *39*(3), 231–238. https://doi.org/10.1080/01616412.2017.1281195

Klimova, B., & Kuca, K. (2015). Alzheimer's disease: Potential preventive, non-invasive, intervention strategies in lowering the risk of cognitive decline–A review study. *Journal of Applied Biomedicine*, *13*(4), 257–261.

Kumar, A., Sidhu, J., Goyal, A., Tsao, J. W., & Doerr, C. (2021). *Alzheimer disease (nursing)*.

Livingston, G., Huntley, J., Sommerlad, A., Ames, D., Ballard, C., Banerjee, S., Brayne, C., Burns, A., Cohen-Mansfield, J., Cooper, C., Costafreda, S. G., Dias, A., Fox, N., Gitlin, L. N., Howard, R., Kales, H. C., Kivimäki, M., Larson, E. B., Ogunniyi, A., … Mukadam, N. (2020). Dementia prevention, intervention, and care: 2020 report of the Lancet Commission. *The Lancet*, *396*(10248), 413–446. https://doi.org/10.1016/S0140-6736(20)30367-6

Livingston, G., Sommerlad, A., Orgeta, V., Jack Jr, C., Bennett, D., Blennow, K., Tricco, A., Ashoor, H., Soobiah, C., & Okura, T. (2019). Current and future treatments in Alzheimer's disease. *Seminars in Neurology*, *39*(02), 227–240.

Lleó, A., Núñez-Llaves, R., Alcolea, D., Chiva, C., Balateu-Paños, D., Colom-Cadena, M., Gomez-Giro, G., Muñoz, L., Querol-Vilaseca, M., Pegueroles, J., Rami, L., Lladó, A., Molinuevo, J. L., Tainta, M., Clarimón, J., Spires-Jones, T., Blesa, R., Fortea, J., Martínez-Lage, P., … Belbin, O. (2019). Changes in Synaptic Proteins Precede Neurodegeneration Markers in Preclinical Alzheimer's Disease Cerebrospinal Fluid. *Molecular & Cellular Proteomics*, *18*(3), 546–560. https://doi.org/10.1074/mcp.RA118.001290

Mansuriya, B. D., & Altintas, Z. (2021). Carbon Dots: Classification, properties, synthesis, characterization, and applications in health care—An updated review (2018–2021). *Nanomaterials*, *11*(10), 2525.

Marzani, B., Balage, M., Vénien, A., Astruc, T., Papet, I., Dardevet, D., & Mosoni, L. (2008). Antioxidant Supplementation Restores Defective Leucine Stimulation of Protein Synthesis in Skeletal Muscle from Old Rats. *The Journal of Nutrition*, *138*(11), 2205–2211. https://doi.org/10.3945/jn.108.094029

Metaxas, A., & Kempf, S. (2016). Neurofibrillary tangles in Alzheimer′s disease: Elucidation of the molecular mechanism by immunohistochemistry and tau protein phospho-proteomics. *Neural Regeneration Research*, *11*(10), 1579. https://doi.org/10.4103/1673-5374.193234

Mosoni, L., Balage, M., Vazeille, E., Combaret, L., Morand, C., Zagol-Ikapitte, I., Boutaud, O., Marzani, B., Papet, I., & Dardevet, D. (2010). Antioxidant supplementation had positive effects in old rat muscle, but through better oxidative status in other organs. *Nutrition*, *26*(11–12), 1157–1162. https://doi.org/10.1016/j.nut.2009.09.016

Nguyen, H. D., Kim, W.-K., & Huong Vu, G. (2024). Molecular mechanisms implicated in protein changes in the Alzheimer's disease human hippocampus. *Mechanisms of Ageing and Development*, *219*, 111930. https://doi.org/10.1016/j.mad.2024.111930

Ordóñez-Gutiérrez, L., & Wandosell, F. (2020). Nanoliposomes as a therapeutic tool for Alzheimer's disease. *Frontiers in Synaptic Neuroscience*, *12*, 20.

Overk, C. R., & Masliah, E. (2014). Pathogenesis of synaptic degeneration in Alzheimer's disease and Lewy body disease. *Biochemical Pharmacology*, *88*(4), 508–516. https://doi.org/10.1016/j.bcp.2014.01.015

Paroni, G., Bisceglia, P., & Seripa, D. (2019). Understanding the Amyloid Hypothesis in Alzheimer's Disease. *Journal of Alzheimer's Disease*, *68*(2), 493–510. https://doi.org/10.3233/JAD-180802

Perl, D. P. (2010). Neuropathology of Alzheimer's Disease. *Mount Sinai Journal of Medicine: A Journal of Translational and Personalized Medicine*, *77*(1), 32–42. https://doi.org/10.1002/msj.20157

Prince, M., Albanese, E., Guerchet, M., & Prina, M. (2014). *World Alzheimer Report 2014. Dementia and Risk Reduction: An analysis of protective and modifiable risk factors.* Alzheimer's Disease International.

Pu, F., Mishima, K., Irie, K., Motohashi, K., Tanaka, Y., Orito, K., Egawa, T., Kitamura, Y., Egashira, N., Iwasaki, K., & Fujiwara, M. (2007). Neuroprotective Effects of Quercetin and Rutin on Spatial Memory Impairment in an 8-Arm Radial Maze Task and Neuronal Death Induced by Repeated Cerebral Ischemia in Rats. *Journal of Pharmacological Sciences*, *104*(4), 329–334. https://doi.org/10.1254/jphs.FP0070247

Qiu, C., Kivipelto, M., & Von Strauss, E. (2009). Epidemiology of Alzheimer's disease: Occurrence, determinants, and strategies toward intervention. *Dialogues in Clinical Neuroscience*, *11*(2), 111–128. https://doi.org/10.31887/DCNS.2009.11.2/cqiu

Richler, J. J., Wilmer, J. B., & Gauthier, I. (2017). General object recognition is specific: Evidence from novel and familiar objects. *Cognition*, *166*, 42–55. https://doi.org/10.1016/j.cognition.2017.05.019

Ricken, F., Can, A. D., Gräber, S., Häusler, M., & Jahnen-Dechent, W. (2022). Post-translational modifications glycosylation and phosphorylation of the major hepatic plasma protein fetuin-A are associated with CNS inflammation in children. *PLOS ONE*, *17*(10), e0268592. https://doi.org/10.1371/journal.pone.0268592

Schaffar, G., Breuer, P., Boteva, R., Behrends, C., Tzvetkov, N., Strippel, N., Sakahira, H., Siegers, K., Hayer-Hartl, M., & Hartl, F. U. (2004). Cellular Toxicity of Polyglutamine Expansion Proteins. *Molecular Cell*, *15*(1), 95–105. https://doi.org/10.1016/j.molcel.2004.06.029

Selkoe, D. J. (2004). Cell biology of protein misfolding: The examples of Alzheimer's and Parkinson's diseases. *Nature Cell Biology*, *6*(11), 1054–1061. https://doi.org/10.1038/ncb1104-1054

Selkoe, D. J., & Hardy, J. (2016). The amyloid hypothesis of Alzheimer's disease at 25 years. *EMBO Molecular Medicine*, *8*(6), 595–608. https://doi.org/10.15252/emmm.201606210

Šimić, G., Babić Leko, M., Wray, S., Harrington, C. R., Delalle, I., Jovanov-Milošević, N., Bažadona, D., Buée, L., De Silva, R., Di Giovanni, G., Wischik, C. M., & Hof, P. R. (2017). Monoaminergic neuropathology in Alzheimer's disease. *Progress in Neurobiology*, *151*, 101–138. https://doi.org/10.1016/j.pneurobio.2016.04.001

Song, N., Sun, S., Chen, K., Wang, Y., Wang, H., Meng, J., Guo, M., Zhang, X.-D., & Zhang, R. (2023). Emerging nanotechnology for Alzheimer's disease: From detection to treatment. *Journal of Controlled Release*, *360*, 392–417. https://doi.org/10.1016/j.jconrel.2023.07.004

Spires-Jones, T. L., & Hyman, B. T. (2014). The Intersection of Amyloid Beta and Tau at Synapses in Alzheimer's Disease. *Neuron*, *82*(4), 756–771. https://doi.org/10.1016/j.neuron.2014.05.004

Sun, X., Chen, W.-D., & Wang, Y.-D. (2015). β-Amyloid: The key peptide in the pathogenesis of Alzheimer's disease. *Frontiers in Pharmacology*, *6*. https://doi.org/10.3389/fphar.2015.00221

Sun, X., Li, L., Dong, Q.-X., Zhu, J., Huang, Y., Hou, S., Yu, X., & Liu, R. (2021). Rutin prevents tau pathology and neuroinflammation in a mouse model of Alzheimer's disease. *Journal of Neuroinflammation*, *18*(1), 131. https://doi.org/10.1186/s12974-021-02182-3

Tatebe, H., Kasai, T., Ohmichi, T., Kishi, Y., Kakeya, T., Waragai, M., Kondo, M., Allsop, D., & Tokuda, T. (2017). Quantification of plasma phosphorylated tau to use as a biomarker for brain Alzheimer pathology: Pilot case-control studies including patients with Alzheimer's disease and down syndrome. *Molecular Neurodegeneration*, *12*(1), 63. https://doi.org/10.1186/s13024-017-0206-8

Tolman, E. C., & Ritchie, B. F. (1943). Correlation between VTE's on a maze and on a visual discrimination apparatus. *Journal of Comparative Psychology*, *36*(2), 91–98. https://doi.org/10.1037/h0062036

Walsh, D., & Selkoe, D. (2004). Oligomers on the Brain: The Emerging Role of Soluble Protein Aggregates in Neurodegeneration. *Protein & Peptide Letters*, *11*(3), 213–228. https://doi.org/10.2174/0929866043407174

Wang, S., Wang, Y.-J., Su, Y., Zhou, W., Yang, S., Zhang, R., Zhao, M., Li, Y., Zhang, Z., & Zhan, D. (2012). Rutin inhibits β-amyloid aggregation and cytotoxicity, attenuates oxidative stress, and decreases the production of nitric oxide and proinflammatory cytokines. *Neurotoxicology*, *33*(3), 482–490.

Wattmo, C., Minthon, L., & Wallin, Å. K. (2016). Mild versus moderate stages of Alzheimer's disease: Three-year outcomes in a routine clinical setting of cholinesterase inhibitor therapy. *Alzheimer's Research & Therapy*, *8*(1), 7. https://doi.org/10.1186/s13195-016-0174-1

Webster, S. J., Bachstetter, A. D., Nelson, P. T., Schmitt, F. A., & Van Eldik, L. J. (2014). Using mice to model Alzheimer's dementia: An overview of the clinical disease and the

preclinical behavioral changes in 10 mouse models. *Frontiers in Genetics*, *5*. https://doi.org/10.3389/fgene.2014.00088

Wiener, H. W., Perry, R. T., Chen, Z., Harrell, L. E., & Go, R. C. P. (2007). A polymorphism in *SOD2* is associated with development of Alzheimer's disease. *Genes, Brain and Behavior*, *6*(8), 770–776. https://doi.org/10.1111/j.1601-183X.2007.00308.x

Wu, L., Xian, X., Xu, G., Tan, Z., Dong, F., Zhang, M., & Zhang, F. (2022). Toll-Like Receptor 4: A Promising Therapeutic Target for Alzheimer's Disease. *Mediators of Inflammation*, *2022*, 1–20. https://doi.org/10.1155/2022/7924199

Xu, P., Wang, S., Yu, X., Su, Y., Wang, T., Zhou, W., Zhang, H., Wang, Y., & Liu, R. (2014). Rutin improves spatial memory in Alzheimer's disease transgenic mice by reducing Aβ oligomer level and attenuating oxidative stress and neuroinflammation. *Behavioural Brain Research*, *264*, 173–180. https://doi.org/10.1016/j.bbr.2014.02.002

Yang, J., Guo, J., & Yuan, J. (2008a). In vitro antioxidant properties of Rutin. *LWT - Food Science and Technology*, *41*(6), 1060–1066. https://doi.org/10.1016/j.lwt.2007.06.010

Yang, J., Guo, J., & Yuan, J. (2008b). In vitro antioxidant properties of Rutin. *LWT - Food Science and Technology*, *41*(6), 1060–1066. https://doi.org/10.1016/j.lwt.2007.06.010

Yiannopoulou, K. G., & Papageorgiou, S. G. (2020). Current and future treatments in Alzheimer disease: An update. *Journal of Central Nervous System Disease*, *12*, 1179573520907397.

Yu, X.-L., Li, Y.-N., Zhang, H., Su, Y.-J., Zhou, W.-W., Zhang, Z.-P., Wang, S.-W., Xu, P.-X., Wang, Y.-J., & Liu, R.-T. (2015). Rutin inhibits amylin-induced neurocytotoxicity and oxidative stress. *Food & Function*, *6*(10), 3296–3306.

Zempel, H., & Mandelkow, E. (2014). Lost after translation: Missorting of Tau protein and consequences for Alzheimer disease. *Trends in Neurosciences*, *37*(12), 721–732. https://doi.org/10.1016/j.tins.2014.08.004

Zenaro, E., Piacentino, G., & Constantin, G. (2017). The blood-brain barrier in Alzheimer's disease. *Neurobiology of Disease*, *107*, 41–56.

Zerrouki, K., Djebli, N., Gadouche, L., Orhan, I. E., Deniz, F. S., & Erdem, S. A. (2021). Protective Effect of Boswellic Resin Against Memory Loss and Alzheimer's Induced by

Aluminum Tetrachloride and D-Galactose (Experimental study in Mice). *Phytothérapie*, *19*(5–6), 306–315. https://doi.org/10.3166/phyto-2020-0222

Zhang, W., Sigdel, G., Mintz, K. J., Seven, E. S., Zhou, Y., Wang, C., & Leblanc, R. M. (2021). Carbon dots: A future Blood–Brain Barrier penetrating nanomedicine and drug nanocarrier. *International Journal of Nanomedicine*, 5003–5016.

Appendices

Appendix A: Composition of Buffers for SDS-PAGE

SDS Lysis Buffer

Sr.No	Components	Quantity g/10ml
1.	SDS	1
2.	50mM Tris-HCl	1.2
3.	10mM EDTA	1.5
4.	Glycerol	1
5.	Protease Inhibitor	1µl
6.	Distilled Water	6.2

1.5M Tris-HCl, pH 8.8 solution

Sr.No	Components	Quantity g/100ml
1.	Tris-HCl	23.64
2.	Distilled water	100

Dissolve tris HCl in 80ml autoclave distilled water. Adjust pH to 8.8 and then add water to make final volume up to 100ml.

1M Tris-HCl, pH 6.8 solution

Sr.No	Components	Quantity g/100ml
1.	Tris-HCl	15.76
2.	Distilled water	100

Dissolve tris HCl in 80ml autoclave distilled water. Adjust pH to 6.8 and then add water to make final volume up to 100ml.

Acrylamide 40%

Sr.No	Components	Quantity g/100ml
1.	Acrylamide	38.67
2.	Bis acrylamide	1.33

3.	Distilled water	100

Dissolve both acrylamide and bis-acrylamide in autoclaved distilled water. Store in brown bottle at 4C°.

10% SDS Solution

Sr.No	Components	Quantity g/10ml
1.	SDS	1
2.	Distilled water	10

10% APS

Sr.No	Components	Quantity g/10ml
1.	APS	1
2.	Distilled water	10

Dissolve APS in water. Prepare fresh after 1 week.

1X Laemmli sample loading buffer

Sr. No.	Components	Quantity 8ml
1.	1M Tris-HCl, pH 6.8	0.4
2.	Glycerol	0.8
3.	10% SDS	1.6
4.	Distilled water	4.8
5.	Bromophenol blue (10%) w/v	20ul
6.	DTT	5

Dissolve all chemicals (1-5) in autoclaved distilled water. Add DTT prior to use. Store at room temperature.

10X SDS-PAGE running buffer, pH 8.3

Sr. No.	Components	Quantity g/100ml

Sr.No.	Components	Quantity
1.	Tris base	3
2.	Glycine	14.4
3.	SDS	1
4.	Distilled water	100

Dissolve all chemicals in autoclaved distilled water. pH should be 8.3 without adjusting. Dilute it to 1X.

Fixative Solution

Sr.No.	Components	Quantity 100 ml
1.	Acetic acid	12
2.	Methanol	50
3.	Distilled water	38

Coomassie Brilliant BlueR250 Staining Solution

Sr.No.	Components	Quantity g/100ml
1.	Acetic acid	12
2.	Methanol	50
3.	Coomassie brilliant blue 250	0.5
4.	Distilled water	38

Add all chemicals to distilled water. Store at room temperature in brown bottle

Destaining Solution

Sr.No.	Components	Quantity g/100ml
1.	Acetic acid	10
2.	Methanol	10
3.	Distilled water	80

Add all chemicals to distilled water. Prepare fresh after 1 week.